MULTI-PLATFORM GEOSPATIAL MODELING OF POTENTIAL EMERALD ASH BORER INFESTATION

A Thesis
Submitted to the Graduate Faculty
of the
North Dakota State University
of Agriculture and Applied Science

By

Samuel George Jenkins

In Partial Fulfillment of the Requirements
for the Degree of
MASTER OF SCIENCE

Major Program:
Environmental and Conservation Sciences

April 2011

Fargo, North Dakota

North Dakota State University
Graduate School

Title

Multi-platform Geospatial Modeling of Potential Emerald Ash Borer Infestation

By

Samuel George Jenkins

The Supervisory Committee certifies that this ***disquisition*** complies with North Dakota State University's regulations and meets the accepted standards for the degree of

MASTER OF SCIENCE

ABSTRACT

Jenkins, Samuel George, M.S., Environmental and Conservation Sciences Program, College of Graduate and Interdisciplinary Studies, North Dakota State University, April 2011. Multi-platform Geospatial Modeling of Potential Emerald Ash Borer Infestation. Major Professor: Dr. Peter Oduor.

This study offers an insight on pertinent parameters that may be considered to address potential emerald ash borer (EAB), *Agrilus planipennis*, infestation. The study utilizes a geospatial model, calibrated using empirical data from Ohio, to model risk of EAB introduction to North Dakota. A spectral library of native trees was also developed to aid in rapid identification of ash tree locations. In light of this imminent threat to North Dakota, a concerted effort to inventory and provide deterministic or stochastic models is critical for providing likelihood scenarios to a consortium of affiliated forest health partners. The premier goal is to mobilize first-responders to alleviate, mitigate or quarantine an affected area and develop plans to minimize the economic impact of an EAB infestation. A cohort study of an existing EAB infestation in Ohio was used to calculate relative risks for proximity to three categories of human infrastructure and ash trees themselves. The relative risks were then used to identify areas in North Dakota that would most be at risk. The results of the risk model show large areas in the eastern part of North Dakota and large swaths of land that have native forest cover, for example, Turtle and Killdeer Mountains, would be most prone to EAB.

ACKNOWLEDGEMENTS

I would like to extend my sincerest gratitude to my academic and thesis advisor Dr. Peter Oduor for guidance and support. I would like to extend thanks to my advisory committee: Drs. Joe Zeleznik, David Rider and Donald Schwert. Major funding was provided from USDA-Forest Service through flow-through funding from North Dakota Forest Service. My sincere appreciation also goes to Jeff Haberman of Fargo Parks and Recreation and the City of Fargo for providing Fargo Street Tree data; Joel Nichols of the North Dakota Forest Service for providing Rural and Community Forest Inventories data; and Bismarck City Forester, Jackson Bird, who provided street tree data for Bismarck, North Dakota. Lastly, I would like to thank my family, Erika, Oliver and Ginny – my lynchpins.

TABLE OF CONTENTS

LIST OF TABLES

LIST OF FIGURES

CHAPTER 1.INTRODUCTION

1.1. Emerald Ash Borer

The emerald ash borer (EAB) is a buprestid beetle which lays its eggs on the bark of ash (*Fraxinus*) trees. Larvae burrow beneath the bark and form galleries where they consume the phloem, girdling and eventually killing a mature tree in 3 – 4 years and younger trees in as little as one year (Poland and McCollough 2006). EAB is native to eastern Asia and was probably introduced to North America via imported ash crating or pallets (Herms, *et al.* 2004). Since its discovery near Detriot, Michigan, in the summer of 2002, EAB has spread rapidly to 13 US states and 2 adjoining Canadian provinces (Emerald Ash Borer 2010).

Three factors make the introduction of EAB to North America a potential natural disaster. First, with no known substantial predators in North America the expansion of the EAB population is largely unrestrained. Second, the unregulated expansion of EAB will have a major impact on the US economy dependent on ash trees and affiliated local economy of areas that would need to be quarantined. There are an estimated 8 billion ash trees in the United States, which make up approximately 7.5% of the volume of hardwood saw timber (Poland and McCollough 2006). In addition, ash is estimated to make up to 14% of the urban leaf area (Sydnor, *et al.* 2007). Loss of this cover will directly impact home summer cooling and winter heating costs. The economic value of urban ash trees across the United States. is estimated at $300 billion (Sydnor, *et al.* 2007). Third, infestation of North American ash trees has a near 100% mortality rate (BenDor, *et al.*

2006), which implies that trees must be replaced to recoup the benefits conferred by the current trees (for example uptake of nutrients especially for riparian forests).

1.2. Objectives

There were two main objectives for this study. The first objective was to develop a spectral library of typical North Dakota forest trees for use in rapid identification of tree species using remote sensing techniques. The second objective was to develop an EAB risk model map for North Dakota in the event of an inadvertent introduction.

1.3. Scope

The geographic focus of this study is the forests of North Dakota. Spectral profiles of forest trees were collected from (a) two North Dakota forest nurseries, and (b) street trees from 2 major urban centers in North Dakota. This may necessitate additional work required to ensure that the spectral library developed accurately models the spectral profiles of trees in other geographic areas. Relative risk models for EAB introduction were calibrated using datasets and in-situ derived data from Ohio and the resulting model was applied to areal extents of North Dakota. There are key assumptions which are further discussed in Section 4.5.

1.4. Organization of Thesis

This thesis presents the findings of studies designed to enhance forest resource and strategic statewide assessment, a stipulated component of the current Farm Bill. The study begins with a review of the current methods of forest mapping, their strengths and weaknesses, current information about the natural history of EAB and efforts to model EAB spread are highlighted in Chapter 2. Chapter 3 outlines the methodology of the spectral library development followed by a qualitative analysis of the variation found in the developed spectral library and the potential amalgamation between library components and orbital or sub-orbital ideal sensor platforms. Finally the development of a spatial technique to identify satellite images for training regions of spectral classification algorithms is ascertained. Chapter 4 discusses the generation of EAB risk maps. It begins by describing the data collection methodology utilized in Ohio and the exposure factors considered. The developed risk model is calibrated thereafter using preliminary Ohio datasets and further discussion offered on comparative EAB risk models. Finally computed relative risks and affiliated demarcated areas are applied to North Dakota in order to generate an affiliated risk map that can be used as a strategic management tool. Sections 4.5 and 4.6 summarize the study findings and recommendations. References and appendices are included at the end of the document.

CHAPTER 2.LITERATURE REVIEW

2.1. Forest Mapping

The USDA requires states to implement comprehensive forest management plans, for continued funding of forest management (Public Law 110 - 234 - Food, Conservation, and Energy Act of 2008. 2008). States must delineate and prioritize forest resources, assess risks, conditions and trends in forests, and develop long-term strategies for managing priority landscapes. Key to a comprehensive management plan is a detailed inventory of the forest resources for each state. There are currently a number of data sets available that map forests.

2.1.1. Current Forest Maps

The stated goal of the United States Geological Survey (USGS) Gap Analysis Program (GAP), born from the realization that a reactionary and piecemeal approach to conservation is an inefficient strategy, is to keep common species common by identifying habitats that are under-represented in conservation lands (Scott 2007). The land cover data are generated primarily from Landsat 5 and digital elevation model data, with a 30m resolution. In total 590 full classes of land cover are defined (Scott 2007). The United States Forest Service (USFS) Forest Inventory and Analysis (FIA) survey is done through on-the-ground survey of trees at random points across the United States (Woodall, *et al.* 2009). The result is a forest map at a 250m resolution that estimates a number of forest parameters. While the data for surveyed points are extremely detailed, the limitations of this technique are the relatively reduced spatial resolution of the images and the lack of precision enforced by interpolation between survey points.

North Dakota is a special case where accurate assessment of forest resources is concerned because of the nature of the distribution of its forests. North Dakota has relatively few densely forested areas, so that much of the existing tree resources consist of small stands of forests, wind breaks and urban forested areas that are rarely mapped on a national scale map.

2.2. Risk Models

Muirhead *et al.* (2006) developed a long distance risk model based upon two scenarios of human-mediated transport of EAB. They used a gravity model to estimate risk. In their approach, they considered proximity to major roads as important conduits for anthropogenically-induced propagation. In the study, population density was used as a proxy for human activities that mediate transportation of EAB beyond the zone of their natural spread. The major drawback with their approach is that factors may exist that contribute to human-mediated spread of EAB, yet are not implicitly associated with population density. For example, one such factor is the likelihood that firewood may be transported to a secluded campground contributing to a long distance introduction of EAB. Another weakness of this methodology is that spread through circular geometric models, while computationally simplistic to program, usually ignores urban transportation models and may fail to predict EAB spread along arterial and other minor connecting roads.

The Minnesota Department of Agriculture (MDA) (2006) developed a risk model for introduction of EAB into Minnesota. The study considered seven factors: (i) campgrounds, (ii) seasonal homes, (iii) urban areas, (iv) sawmills, (v) firewood, (vi) nurseries, and (vii) accessibility. Where numerical data were available, an assessment of the importance of each factor was made on an arbitrary scale of 1 – 1,000. Risks for each factor were classified into 256 equally sized bins and combined according to a regression equation that produced spatial results that matched the expectations of MDA officials.

Ayersman *et al.* (2009) present an EAB risk model for an area encompassing six states based on three risk factors: campgrounds, nurseries and sawmills. Their analysis was based on density calculations of each equally weighted industry. On the other hand, Prasad *et al.* (2010) used a more comprehensive model to predict the spread of EAB in Ohio. Their model combines two recognized methods of EAB spread: (i) an insect flight model, which models natural spread of the insect; and (ii) an insect ride model, which models long distance, human facilitated spread of EAB. The factors considered important in the insect ride model are traffic on roads, wood products industries, population density and campgrounds. Within each factor an increasing, but arbitrary, weight was applied to areas thought to pose more risk, such as roads with increased traffic density, campgrounds with more sites, wood product industries which handled large volumes of ash. Scores for each risk factor were weighted (60% for roads, 20% for campgrounds, 10% for wood products industries and 10% for population density) and the final score used as a multiplier of ash basal area to produce a final risk map.

CHAPTER 3. SPECTRAL LIBRARY DEVELOPMENT

3.1. Introduction

An important step in identifying an object in a remotely sensed image is to have an accurate assessment of the spectral characteristics of the object so that corresponding image pixels with those characteristics may be selected. With this goal in mind, a spectral library of trees and shrubs typical in North Dakota forests was developed.

3.2. Generation of Spectral Library of North Dakota Forest Trees

An ASD Inc. Field SpecPro® spectrometer with leaf clip assembly was used to generate the spectral library. In the very near infra-red (VNIR) wavelength range, 350 – 1000 nm, an individual detector for each measured wavelength is positioned to receive light within a 1.4 nm bandwidth. The VNIR spectrometer has a spectral resolution of approximately 3 nm at around 700 nm. In the near infra-red (NIR) wavelength range, 900 – 2500 nm, there are two detectors, which are exposed to different wavelengths of light as a grating oscillates. The first detector measures light between about 900 – 1850 nm; the second covers the 1700 - 2500 nm region. The spectral resolution in the NIR range varies between 10 nm and 12 nm, depending on the scan angle at that wavelength.

The spectral library, constructed during the first three weeks of July 2009, comprises a snapshot of potential leaf spectra which coincides with leaf maturity and a full leaf canopy for typical North Dakota trees and forests. Spectral samples were obtained at Lincoln Oakes Nursery, Bismarck, which is run by North Dakota Association of Soil Conservation Districts and Towner State Nursery, Towner, which is run by North Dakota

Forest Service. Replicate samples were collected *in situ* (when leaves were attached to the tree; Figure 1) and *ex situ* (after the leaves had been stored overnight; Figure 2) to gauge change in spectral indices. Each sample was scanned at least four different times on different leaves, with each scan being the average of 25 detector readings. Samples were wrapped in paper towels, bagged in plastic storage bags and stored overnight in a cooler. Stored samples were scanned, the following day, at least eight different times on different leaves. No observable difference was seen between spectral profiles taken from leaves on the plant, immediately taken from the plant or stored overnight. The spectral library contains 963 spectral profiles composed of 29 genera and 53 species. The entire distribution is shown in Appendix A.

Figure 1. Field data collection

Figure 2. Laboratory set-up of the ASD Field SpecPro®

3.3. Analysis of Spectral Library Variation

To examine the variability of spectral profiles the spectral angle (α) between each pair of profiles was calculated using the formula shown below (Research Systems 2003):

$$\alpha = \cos^{-1}\left[\frac{\sum_{i=1}^{n} t_i r_i}{\sqrt{\left(\sum_{i=1}^{n} t_i^2\right)}\sqrt{\left(\sum_{i=1}^{n} r_i^2\right)}}\right], \tag{3.1}$$

where t is test spectrum and r is a reference spectrum. Spectral Angle algorithm measures the cumulative differences in reflectance between the test and reference spectrum at each available wavelength. The smaller the spectral angle, the more closely related are the two spectra. The results from this study were displayed as a simulated correlation matrix

(Figure 3). Each spectral profile in the library is represented along the x-axis (test spectra) and repeated down the y-axis (reference spectra). The result is that the diagonal pairs have the same test and reference spectra, so the calculated spectral angle is always zero (represented by a dark blue color). Spectral angle in this library ranged from 0 to 0.778. The largest spectral angles, occurring primarily between coniferous and deciduous leaves are shown in a reddish-brown color. The larger, labeled boxes on the diagonal delineate spectra that belong to leaves from the same genus. The smaller boxes within genus boundaries delineate spectra that belong to the same species.

Figure 4 shows a generalized form of Figure 3 derived by averaging the spectral angle values for each test/reference pair combination within a genus and classifying by quantile. With this technique variation within a genus and amongst different genera can be more easily assessed.

Table 1 describes the variation in spectral angle amongst profiles from the same genus. Genera such as poplar (*Populus*), ash (*Fraxinus*) and linden (*Tilia*) have a low average spectral angle, indicating that one poplar, ash or linden tree looks much like another. Pines (*Pinus*) have a much higher within-genus spectral angle. The conifers, pines, spruce and, to a lesser extent, junipers are easily distinguishable from deciduous trees, and less distinguishable amongst themselves. Table 1 is color coded with the colors assigned to spectral angle in Figure 4 and ordered by increasing mean spectral angle. Various instrumentation calibrations were performed, for example, instrument optimization to adjust instrument sensitivity was performed automatically for every sample measurement. This is a necessary step to ensure that changing levels of down welling

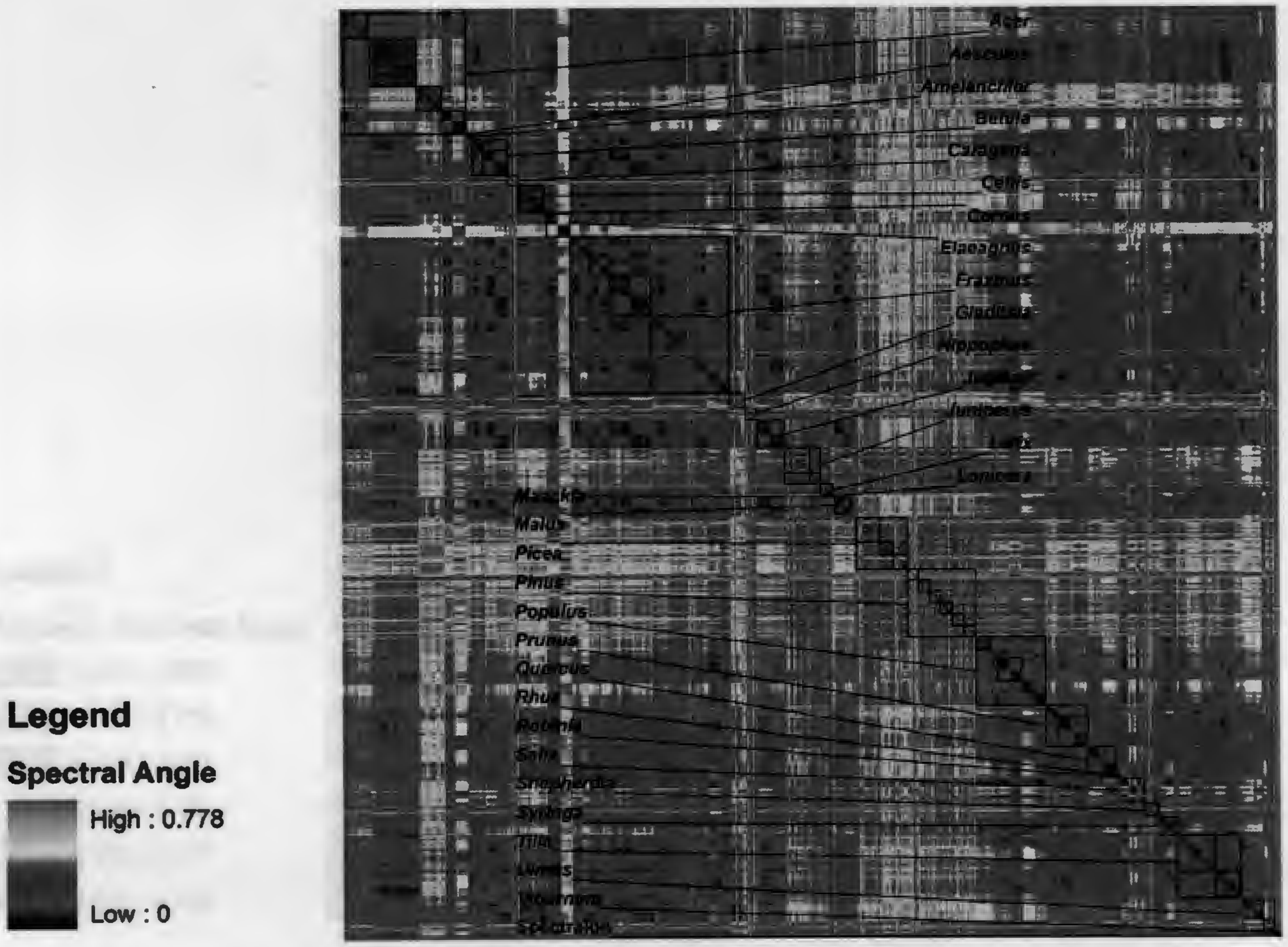

Figure 3. Spectral library spectral angle correlation matrix

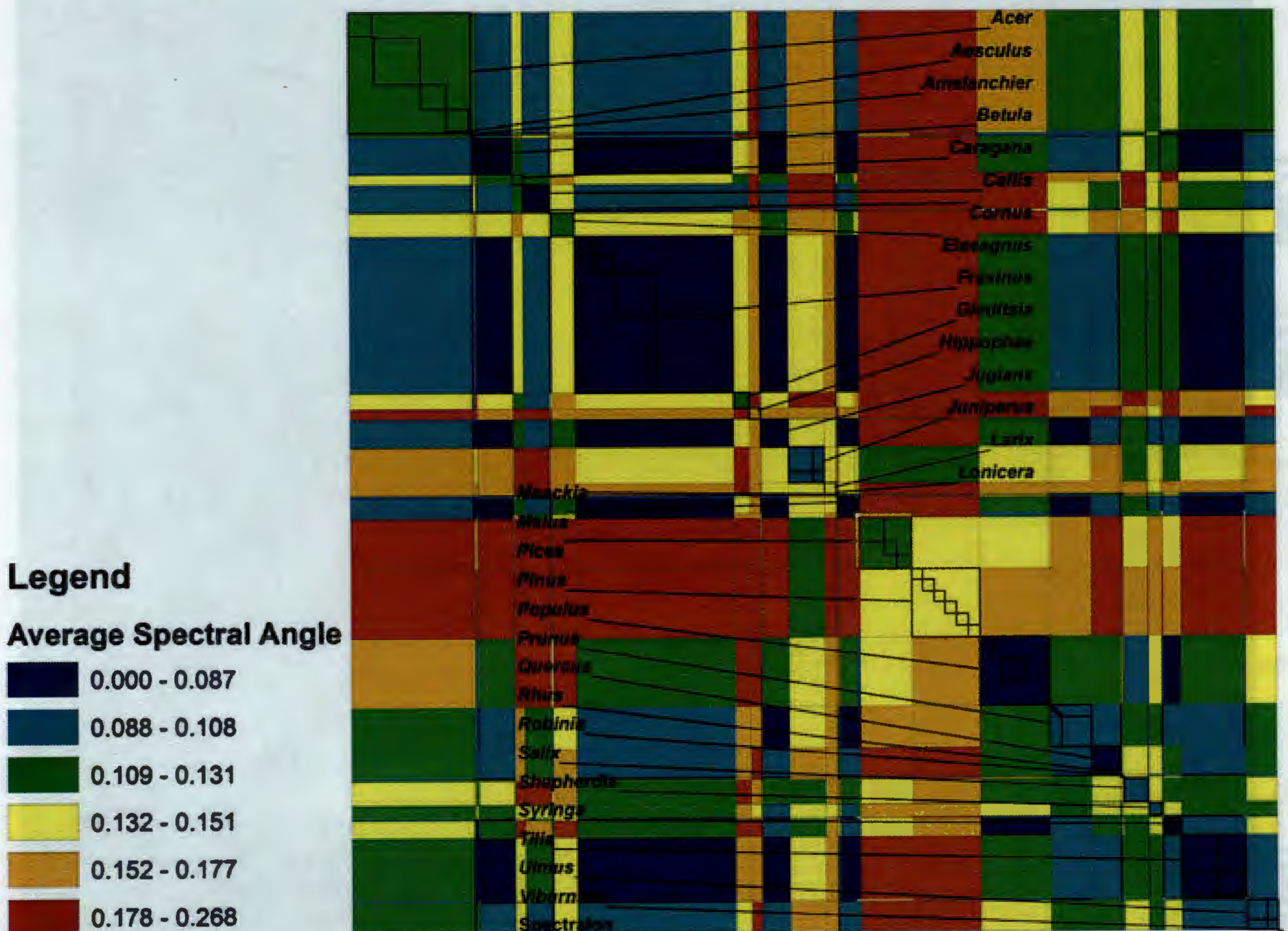

Figure 4. Average spectral angles for genera

Table 1. Spectral angle genus summary table

			Spectral Angle		
Genus	Profile Count	Species Count	Maximum	Mean	Standard Deviation
Lonicera	1	1	0	0	0
Viburnum	1	1	0	0	0
Maackia	4	1	0.014	0.007	0.008
Rhus	4	1	0.043	0.021	0.025
Aesculus	4	1	0.046	0.023	0.026
Cornus	4	1	0.056	0.028	0.032
Celtis	729	1	0.114	0.039	0.020
Juglans	784	1	0.097	0.046	0.025
Malus	256	1	0.110	0.053	0.031
Betula	1296	2	0.143	0.062	0.030
Amelanchier	9	1	0.118	0.062	0.051
Populus	5184	2	0.186	0.067	0.034
Syringa	324	4	0.151	0.069	0.037
Fraxinus	26569	4	0.286	0.077	0.038
Robinia	4	1	0.156	0.078	0.090
Tilia	4225	3	0.202	0.081	0.038
Quercus	841	1	0.186	0.084	0.047
Prunus	1849	6	0.226	0.088	0.044
Juniperus	1369	2	0.354	0.093	0.065
Salix	625	1	0.236	0.100	0.068
Ulmus	1024	1	0.319	0.101	0.070
Shepherdia	169	1	0.304	0.101	0.077
Acer	15625	4	0.283	0.112	0.063

Table 1 (continued)

			Spectral Angle		
Genus	Profile Count	Species Count	Maximum	Mean	Standard Deviation
Gleditsia	256	1	0.308	0.117	0.085
Picea	2809	3	0.383	0.119	0.084
Caragana	100	1	0.299	0.125	0.085
Elaeagnus	576	1	0.294	0.127	0.100
Pinus	4900	6	0.593	0.149	0.120
Larix	144	1	0.425	0.151	0.133
Hippophae	121	1	0.478	0.169	0.131

irradiance do not cause the instrument detectors to saturate. Dark current, amount of electrical current generated by electrons within the instrument, was eliminated from base profiles by periodic optimization. The spectral response of the target (leaves) was then automatically computed by dividing its spectral response by that of the reference sample (spectralon).

Figure 5 shows variation in spectral angle within a test/reference genera pairing. Within genus is typically low (< 0.039). Notable exceptions are the pine (*Pinus*) and spruce (*Picea*) needles (> 0.072))which are very difficult to scan with the leaf clip, as evidenced by the large standard deviation.

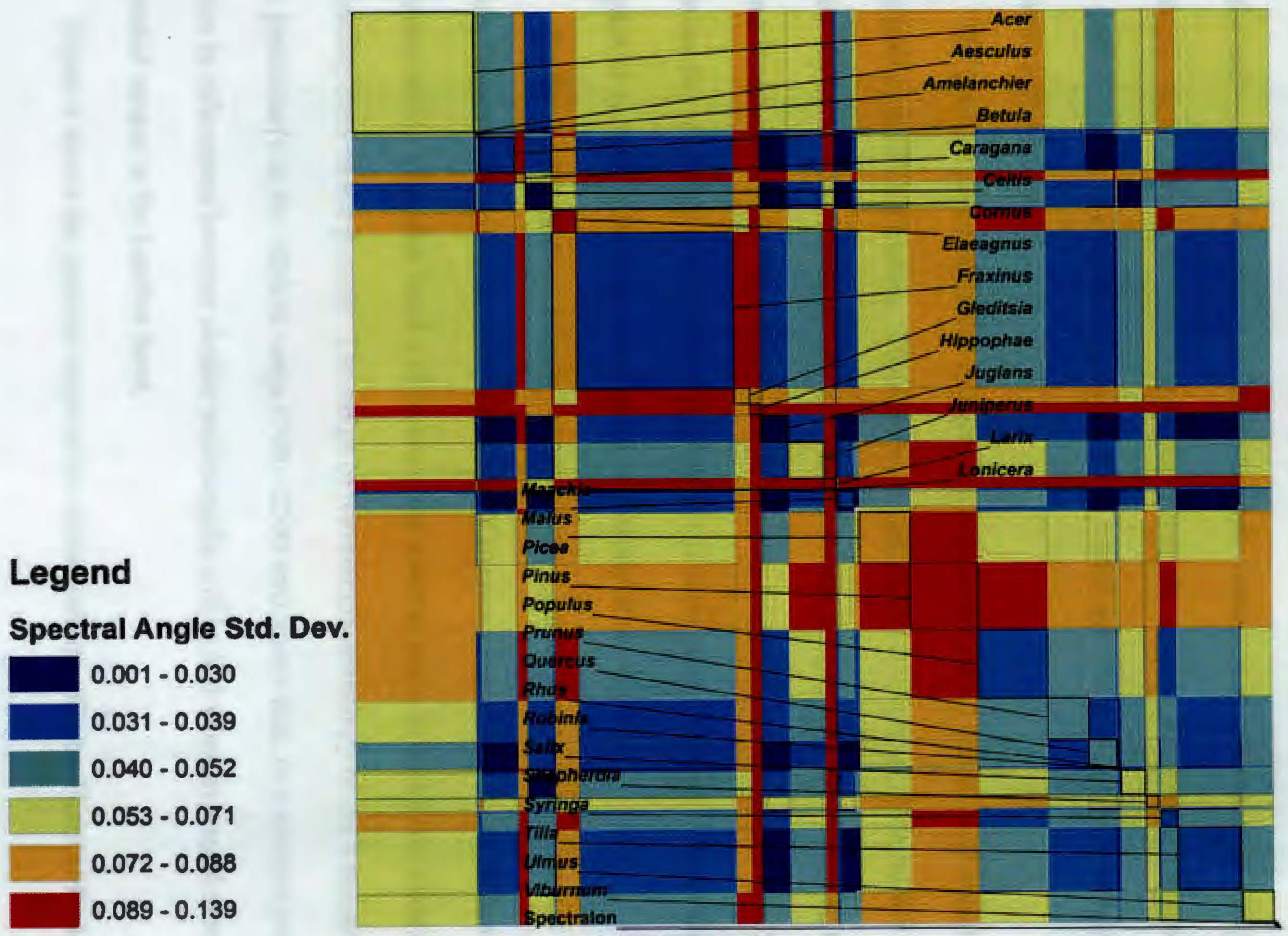

Figure 5. Variation of spectral angles within genera

3.4. Analysis of Spectral Coverage of Remote Detectors

Figure 6 was used to elucidate optimum orbital scanners whose imagery would provide the best spectral resolution. Figure 6 was created by averaging the reflectance value for each profile in a genus at each wavelength. Variation in reflectance at each wavelength can be seen in the variation of hue among the genera. Regions of the spectra which contain variation among the genera will be useful wavelengths at which to harness reflectance information.

The Landsat series of orbital imagers are a commonly used orbital land imaging device with a significant history. The relatively high revisit frequency (16 days) and its large survey area, with a swath of 185 km, make Landsat images attractive mapping tools (Landsat Handbook 2008). The drawbacks of Landsat images for forest mapping in North Dakota are the relatively coarse spatial resolution (Landsat pixels measure 30m x 30m), the large gaps in spectral information and broad sensitivity of the detectors.

The black rectangles on Figure 7 represent the spectral ranges of the Landsat Enhance Thematic Mapper plus (ETM+) bands. Variation among reflectance values in each genus within a Landsat band will increase the spectral angle between two pixels representing trees on the ground. The range of wavelength sensitivity of the Landsat bands, particularly in the infrared range (700 – 2500 nm) means that, in a spectral profile, variation in reflectance between similar wavelengths will be lost when averaged over all the spectral ranges in the Landsat band.

Figure 8 shows the spectral range of the Advanced Spaceborne Thermal Emission

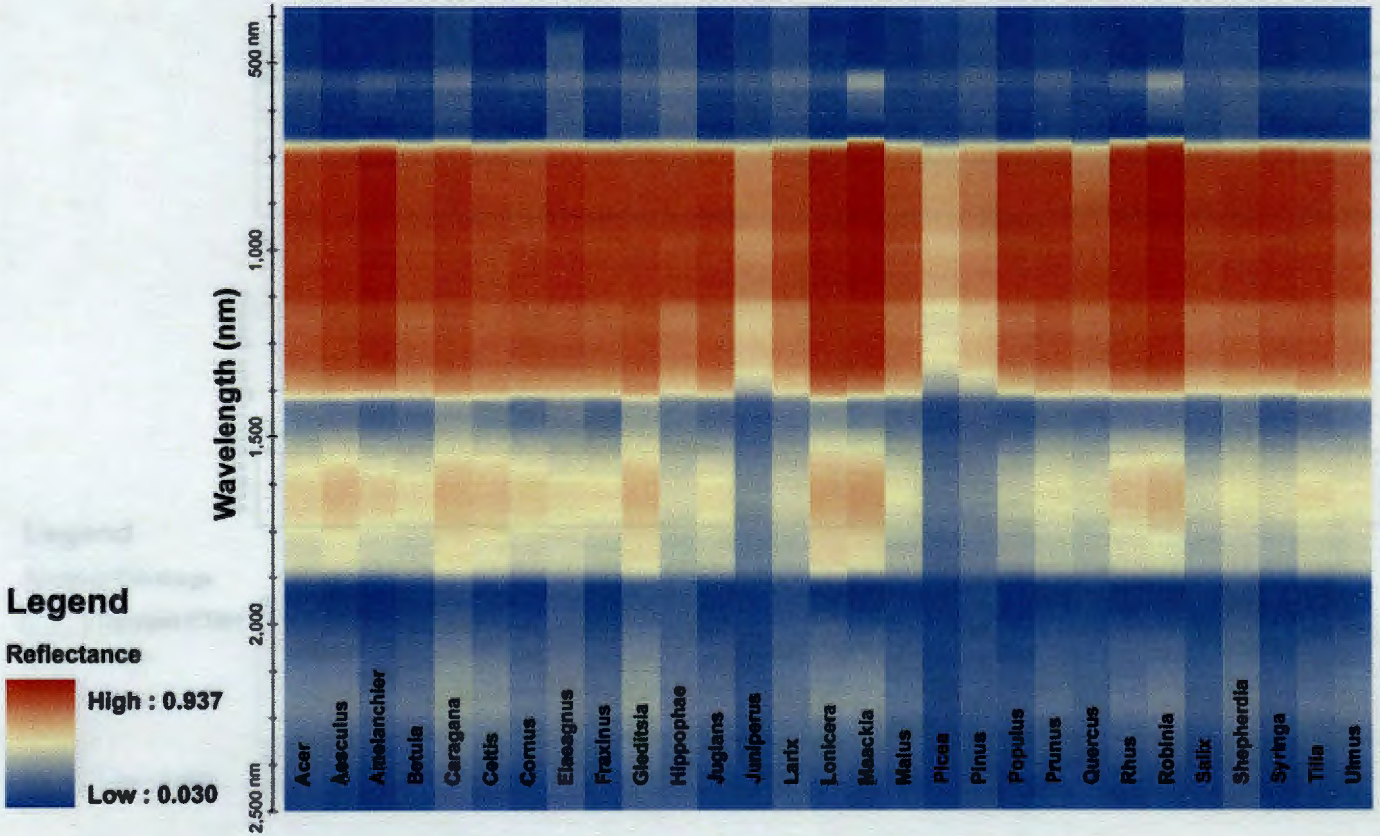

Figure 6. Genus reflectance variation by wavelength

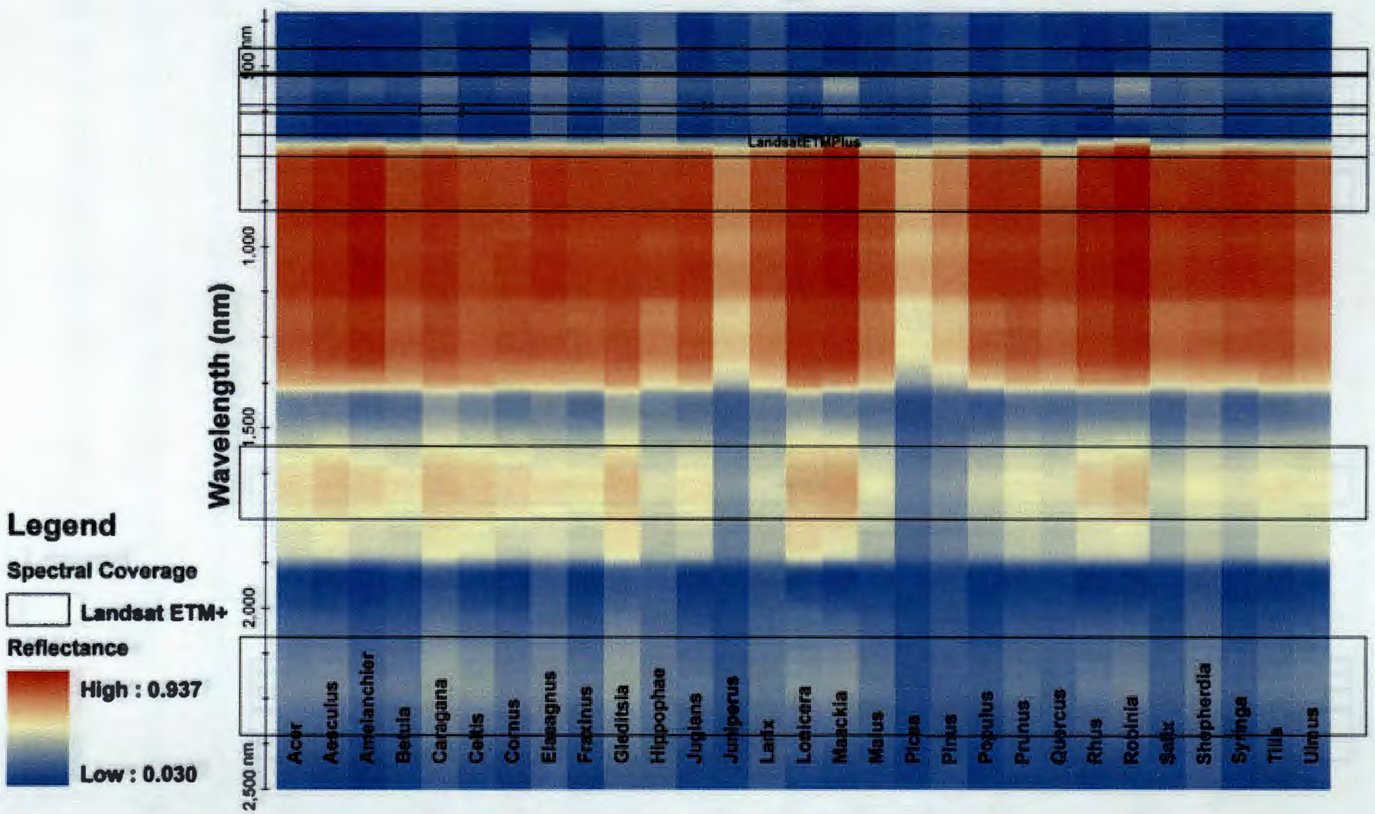

Figure 7. Spectral coverage of Landsat 7 (Data from Landsat Handbook 2008)

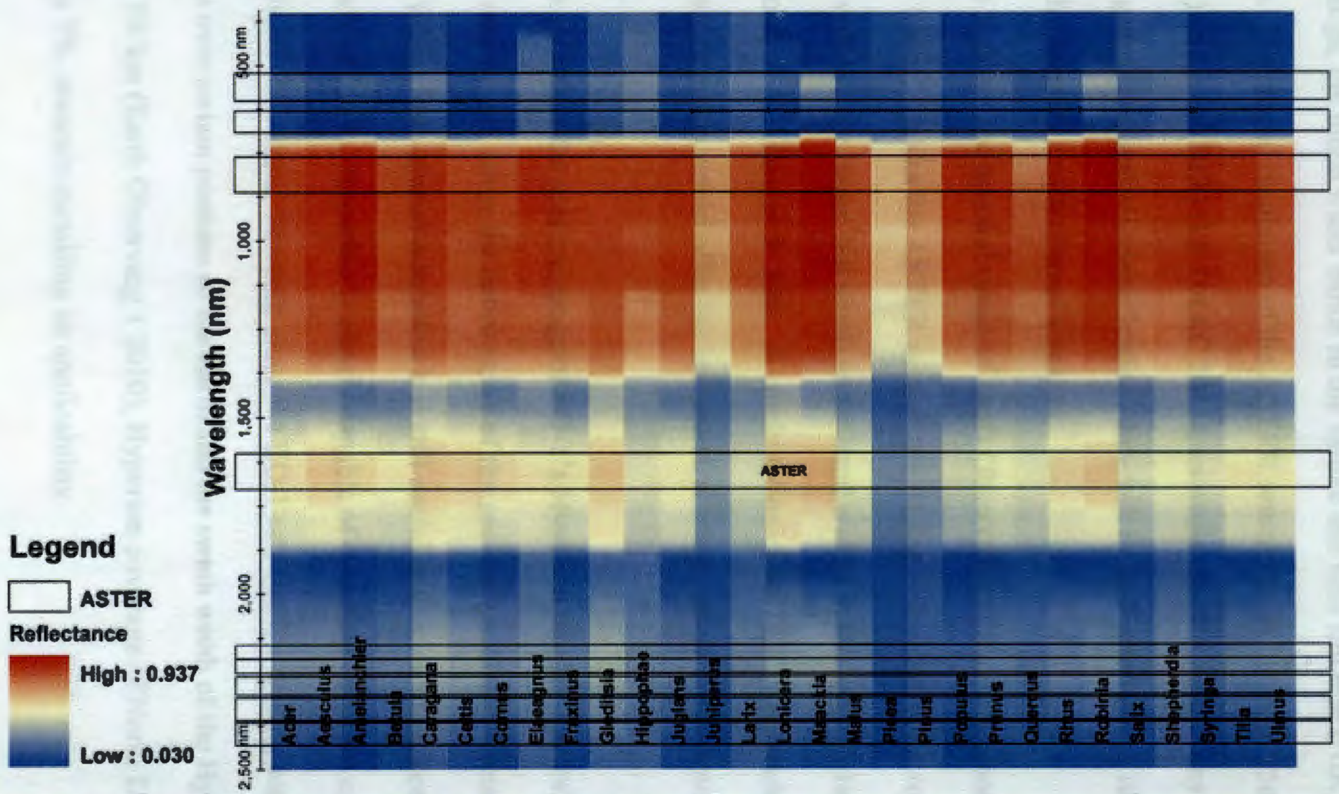

Figure 8. Spectral coverage of ASTER (Data from LP DAAC 2011)

and Reflection radiometer (ASTER) bands. Variation within each ASTER band will contribute to a low α value (from Eq. 3.1). The ASTER sensor contains narrow bands in the infrared range, but much wider bands in the visible and near Infrared (NIR) bands (LP DAAC 2011). The spatial resolution of the ASTER sensor varies between 15m (visible and very NIR) and 90m (NIR) (LP DAAC 2011), so while the NIR bands may be applicable to genera and species identification; they will be of limited use in identifying much of North Dakota's smaller forest acreages.

Figure 9 shows the spectral range of Earth Observing (EO) -1's Advanced Land Imager (ALI) bands. Unlike the ASTER sensor, the ALI sensor contains narrow band widths in the visible light range, but much wider band widths in the infrared region. The spatial resolution of ALI images is 30m. A combination of ASTER NIR bands and ALI visible wavelength bands would offer the best spectral combination to maximize ash tree identification.

Figure 10 shows the spectral range of EO-1's Hyperion bands. The 242 bands of Hyperion are narrow and cover the entire range of the spectral profiles collected for ND tree species. With a 30m spatial resolution it is still useful in species identification in moderate stands of forest. Hyperion is clearly capable of detecting variation contained in the spectral library developed; however since the EO-1 satellite is a tasking satellite with limited passes over certain portions of the Earth and the swath width of the Hyperion sensor is just 7.6 km (Earth Observing 1 2010), Hyperion coverage of North Dakota is only approximately 7%, severely curtailing its applicability.

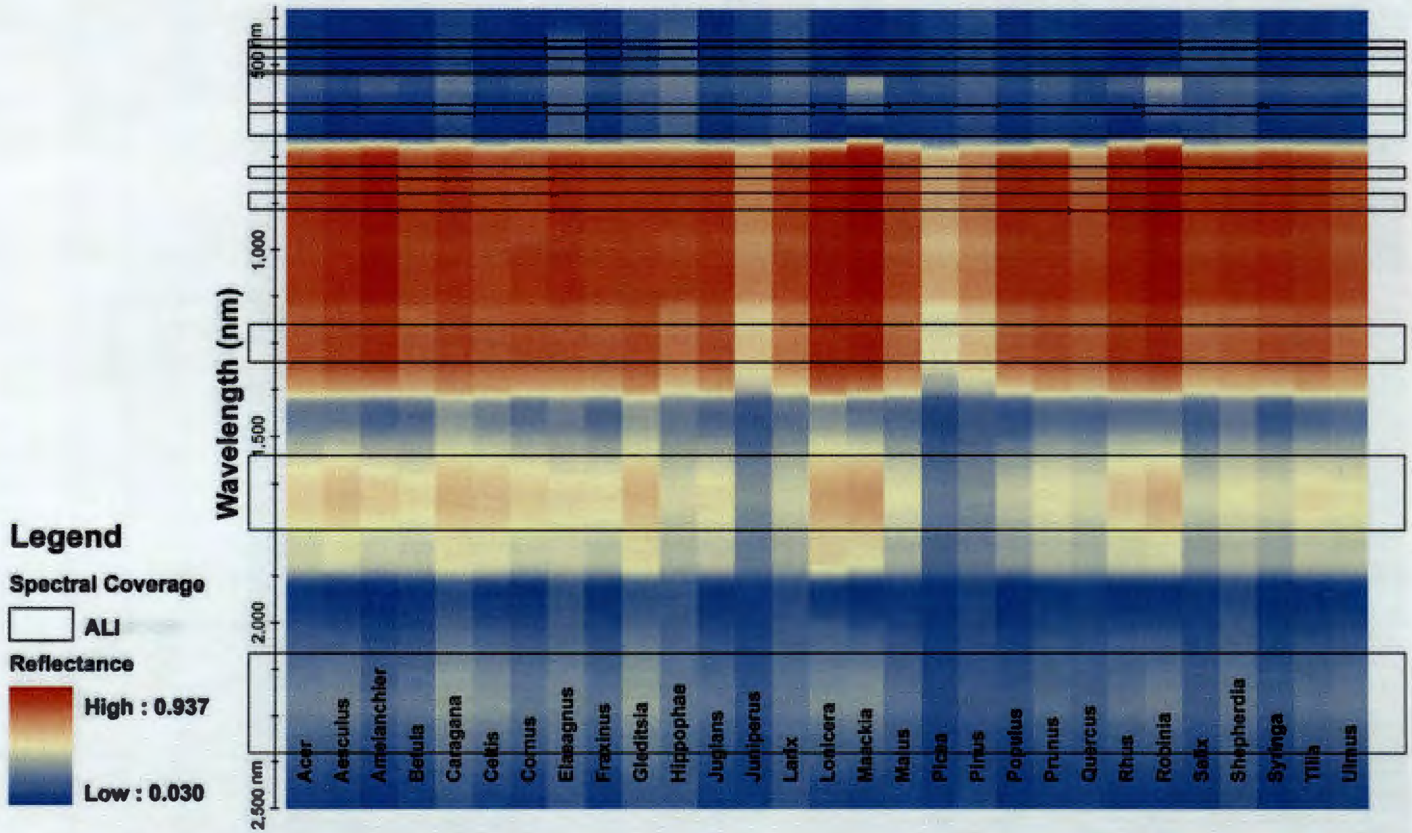

Figure 9. Spectral coverage of EO-1 ALI (Data from Earth Observing 1 2010)

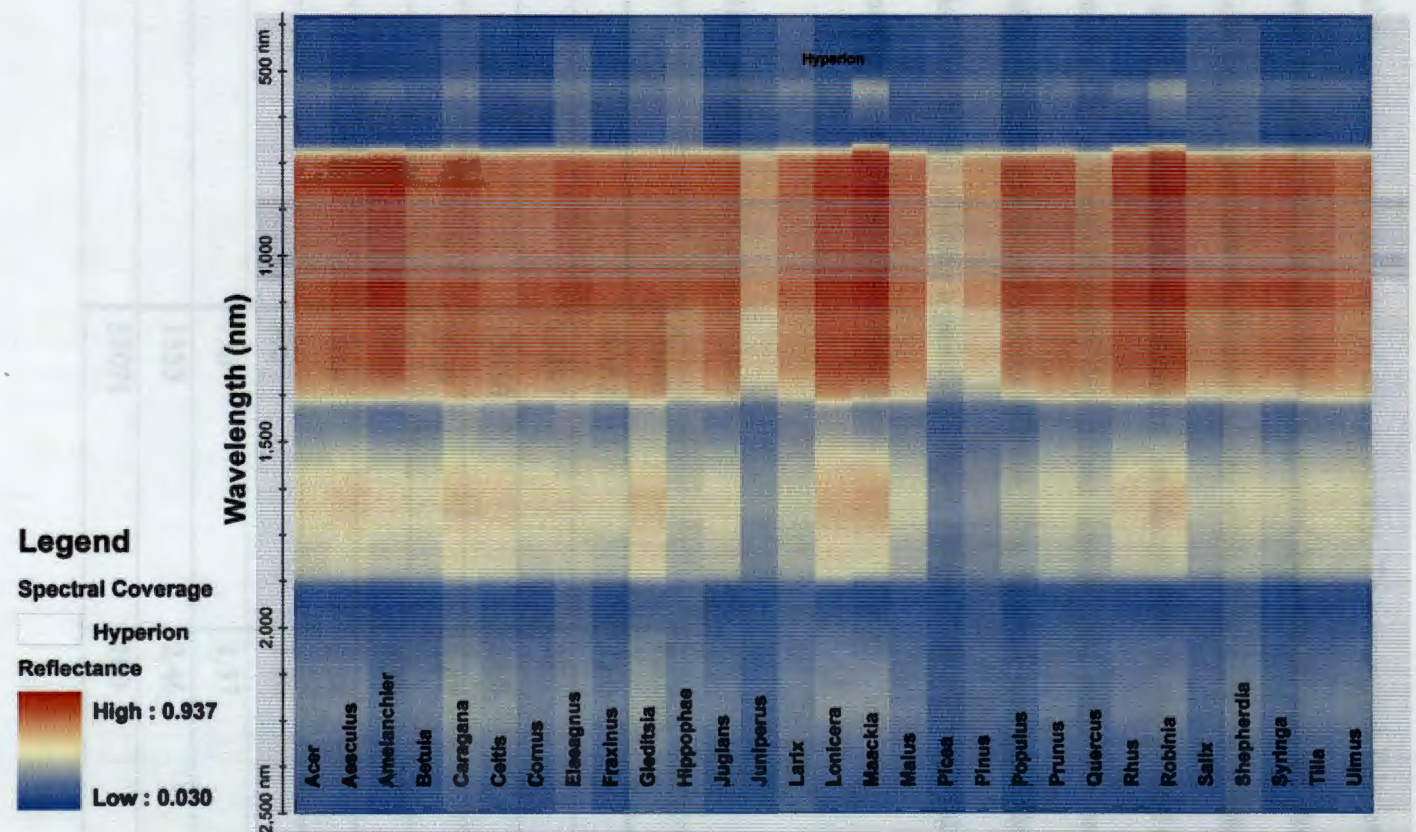

Figure 10. Spectral coverage of EO-1 Hyperion (Data from Earth Observing 1 2010)

3.5. Identification of Training Datasets for Image Classification

When using remotely sensed data to ascertain land cover or land use categories it is also essential to provide some estimate of data accuracy. To accomplish this, estimation training datasets were derived, for which on-the-ground data already existed. Images containing both high proportions of ash tree-crowns and high proportions of other likely tree-crowns were processed as training datasets. In March 2009 on-the-ground data were obtained from the City of Fargo Forestry department (unpublished data). Records include the street address and the genus and species of trees. The database was geocoded using the street address of each tree, yielding a point data layer, *Fargo_Street_Trees*. Table 2 shows a summary of the *Fargo_Street_Trees* data layer.

Table 2. Listing of Fargo street trees by genus

Genus	Count	Percent
Fraxinus	18152	33.0
Unknown	15497	28.1
Ulmus	13650	24.8
Acer	2020	3.67
Tilia	1818	3.30
Celtis	1016	1.84
Prunus	805	1.46
Malus	758	1.37
Other	1355	2.46
Total	55071	100

Ash trees are hardy, fast growing, drought and alkali tolerant (Herman and Chaput 2003). They are seen throughout the cities of Fargo and West Fargo where they have been planted over the last half century as new and replacement trees (Figure 11). The other notable genus present as Fargo street trees is *Ulmus* (elms). Before the onset of Dutch elm disease which reached the Midwest during the latter half of the 20th century, elms were a common street tree (Herman and Chaput 2003). The bulk of the elms in Fargo are seen in the older neighborhoods around downtown and towards the north (Figure 11). A third category of trees in the database did not have a recorded genus. These are distributed in a manner more like the distribution of ash trees than elms and probably represent ash trees or other genera in the proportions shown in the rest of the database (Figure 11).

A data layer (*Fargo_Street_Trees_Fraxinus*) containing the location of *Fraxinus* tree species in Fargo was produced from the *Fargo_Street_Trees* data layer, by selecting *Fraxinus* from the genus attribute table and exporting the selected points (Table 3).

Table 3. Make-up of *Fraxinus* street trees by species

Species	Count	Percent
Unknown	6	0.033
F. americana	172	0.948
F. nigra X *F. mandshurica*	186	1.02
F. mandshurica	708	3.90
F. nigra	1350	7.44
F. pennsylvanica	15730	86.7
Total	18152	100

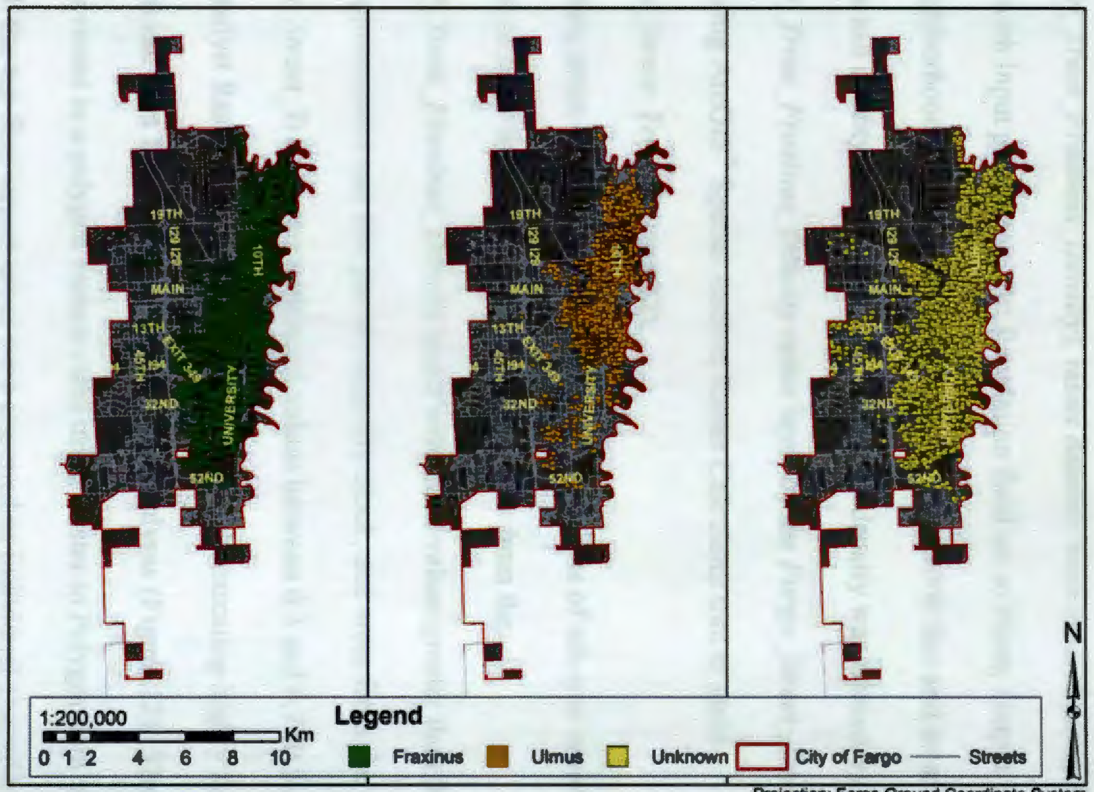

Figure 11. City of Fargo tree inventory (Data from City of Fargo Forestry, unpublished data)

The *Fargo_Street_Trees_Fraxinus* layer shows that the most commonly planted tree is the green ash (*F. pennsylvanica*). It is the hardiest of the ash species and comes in a multitude of cultivars (Herman and Chaput 2003).

Total tree density (*Fargo_Street_Trees_Density*), and ash tree density (*Fargo_Street_Trees_Fraxinus_Density*), raster datasets were created using ArcGIS® Point Density tool with input parameters for: Population field set to None, Output cell size set to 100 feet, Neighborhood geometry set to a circle of radius 1000 feet and areal units of acres selected. The ash density as a percentage of total tree density was educed by dividing *Fargo_Street_Trees_Fraxinus_Density* raster layer by the *Fargo_Street_Trees_Density* raster layer using ArcGIS® Spatial Analyst Raster Calculator tool to yield *Pct_Fraxinus_Street_Trees* (Figure 12).

Selecting areas containing both adequate proportions of ash-tree crowns and a range of tree crowns of other was achieved by selecting areas from the *Fargo_Street_Trees_Fraxinus_Density* raster with pixel values greater than 8.17 trees/acre, a value that approximates one tree per average city block, and areas from the *Pct_Fraxinus_Street_Trees* raster with pixel values between 0.3 and 0.7 (0.5 ± 0.2), using the Spatial Analyst Raster Calculator tool. This aids in demarcating highly forested regions with sufficient ash trees for training and distinction analyses (Figure 12). The weighted raster was converted to a polygon feature class using Raster to Polygon tool and the polygons with the top-four largest areas were exported as individual shapefiles. Coordinates of each polygon centroid was determined. The extent and centroid of each of the four shapefiles was used as base areal extents to derive training data limits (Appendix B).

CHAPTER 4. EMERALD ASH BORER RISK MAP DEVELOPMENT

4.1. Introduction

Given the potential for destruction posed by EAB it is essential that areas currently unaffected prepare adequately to protect their ash resources. This preparation begins with identifying those areas most at risk of EAB introduction. North Dakota has an estimated 78.1 million ash trees (Haugen, *et al.* 2005) and, with EAB discovered in southern Minnesota in May 2009 (MDA 2009), it is imperative that a management plan to protect those resources be put in place. The process outlined in this chapter describes the application of a method of quantifying the risks not previously reported in work associated with introduction of EAB. Previously, analysis of the risk of introduction has been based upon educated estimations of importance of factors (Prasad, *et al.* 2010) and (MDA 2006). This method uses an epidemiological cohort study analysis to determine appropriate weighting across factors to get a more accurate assessment of overall risk. Four factors known to be associated with introduction of EAB to previously unaffected areas – proximity to existing ash stands, campgrounds, roads and rails – are addressed.

4.2. Cohort Data

The Ohio Department of Agriculture began monitoring EAB in 2005, after early cases were discovered in 2003 and 2004 (Prasad, *et al.* 2010). In 2005, 'detection trees,' 18 from each Ohio township, were girdled to make them more attractive to EAB. During the months following the 2005 growing season half of the detection trees were removed and inspected for EAB larvae underneath the bark (Prasad, *et al.* 2010). The remainder of the 'detection trees' were removed and inspected following the 2006 growing season. Data for 10,176 detection trees were obtained from United States Forest Service, Northern Research Station (personal communication, Anantha Prasad). The data mapped the location of detection trees, set up in 2005 and 2006 and those trees that yielded EAB larvae at the time of removal (Figure 13).

4.2.1. Calibration Data

The data obtained for calibrating the model developed constituted an epidemiological cohort study, from which relative risks for various exposure factors can be calculated (e.g. Lerner and Kannel 1986; Alberman *et. al.* 1971). Relative risks are defined as the ratio of the probability of cases in the exposure class to the probability of cases in the unexposed class. It has been suggested in previous studies (e.g. Prasad, *et al.* 2010; MDA 2006) that introduction of EAB to new areas is primarily facilitated by humans. While EAB does spread naturally, its rate of movement has been estimated at less than 20 km per year (Prasad, *et al.* 2010), well below the rates required to account for current distribution patterns. For this reason, foresters and entomologists have identified likely methods of spread associated with human activity (Prasad, *et al.* 2010). In this study, campgrounds, roads, rails and ash tree density were assessed as primary source factors due to their prevalence as exposure pathways from numerous studies.

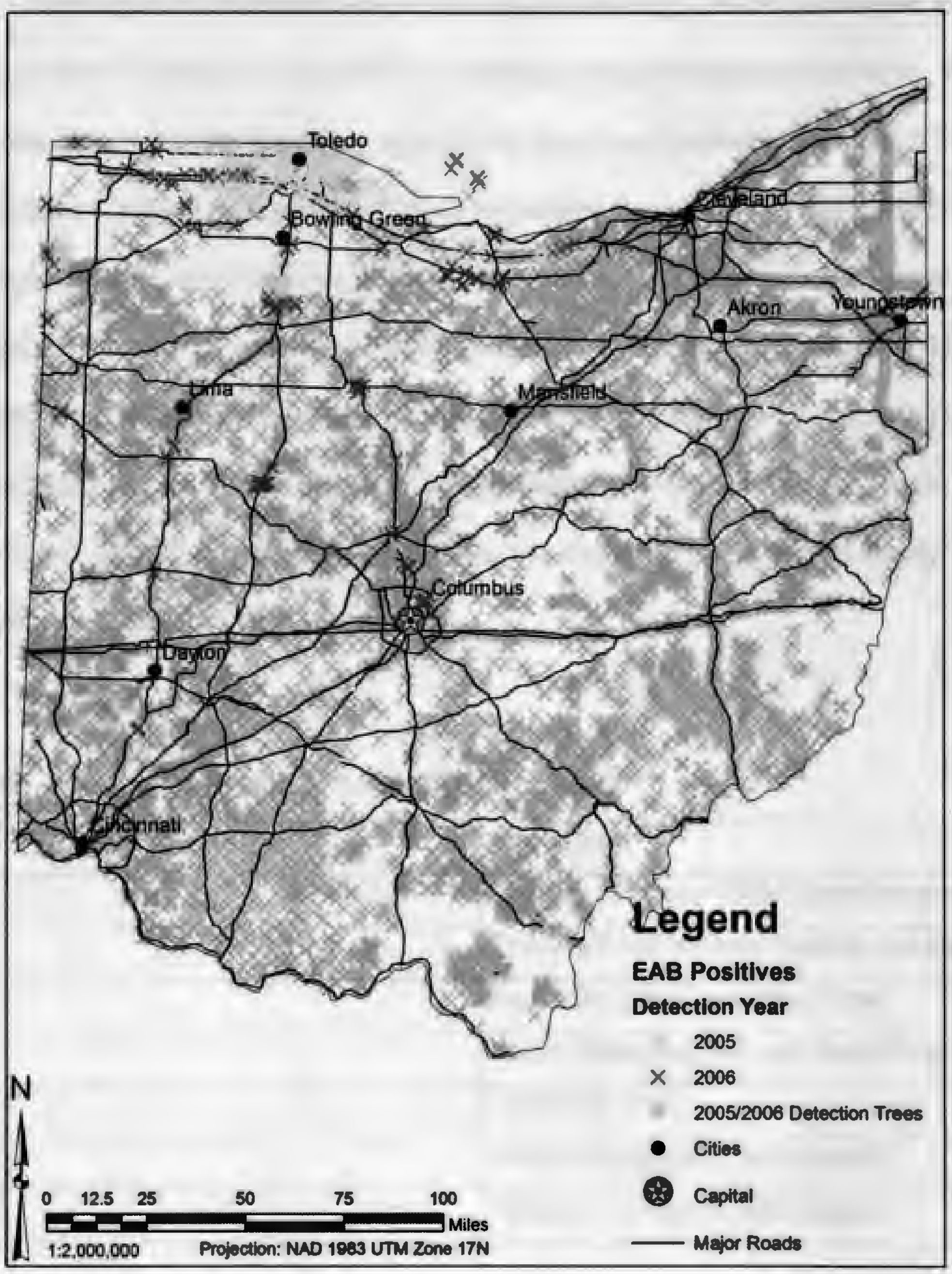

Figure 13. Distribution of EAB detection trees and EAB positive ash trees (Data from Ohio Department of Agriculture)

4.2.2. Exposure to Roads

Topologically Integrated Geographic and Referencing (TIGER) road centerline files (Census 2000 TIGER/Line Data 2000) were used as vehicular transportation input. Each road was categorized based on type, according to the Census Feature Class Code (CFCC) descriptions (Table 4). Increasing CFCC codes denotes decreasing carrying capacity, although no traffic count data was factored in this study. Proximity to each category except A4 and A6 was used as an exposure factor in calculation of relative risks (Figure 14). The A4 category was excluded because each detection tree and confirmed EAB positive was within 2 km of a road in this category, implying that a "no exposure" category could not be established. The A6 category was also excluded as it contains roads without clearly definable characteristics.

Table 4. Census Feature Class Codes (CFCC) for roads

CFCC	Description
A1	Primary Highway With Limited Access
A2	Primary Road Without Limited Access
A3	Secondary and Connecting Road
A4	Local, Neighborhood, and Rural Road
A5	Vehicular Trail
A6	Road with Special Characteristics
A71	Walkway or trail for pedestrians

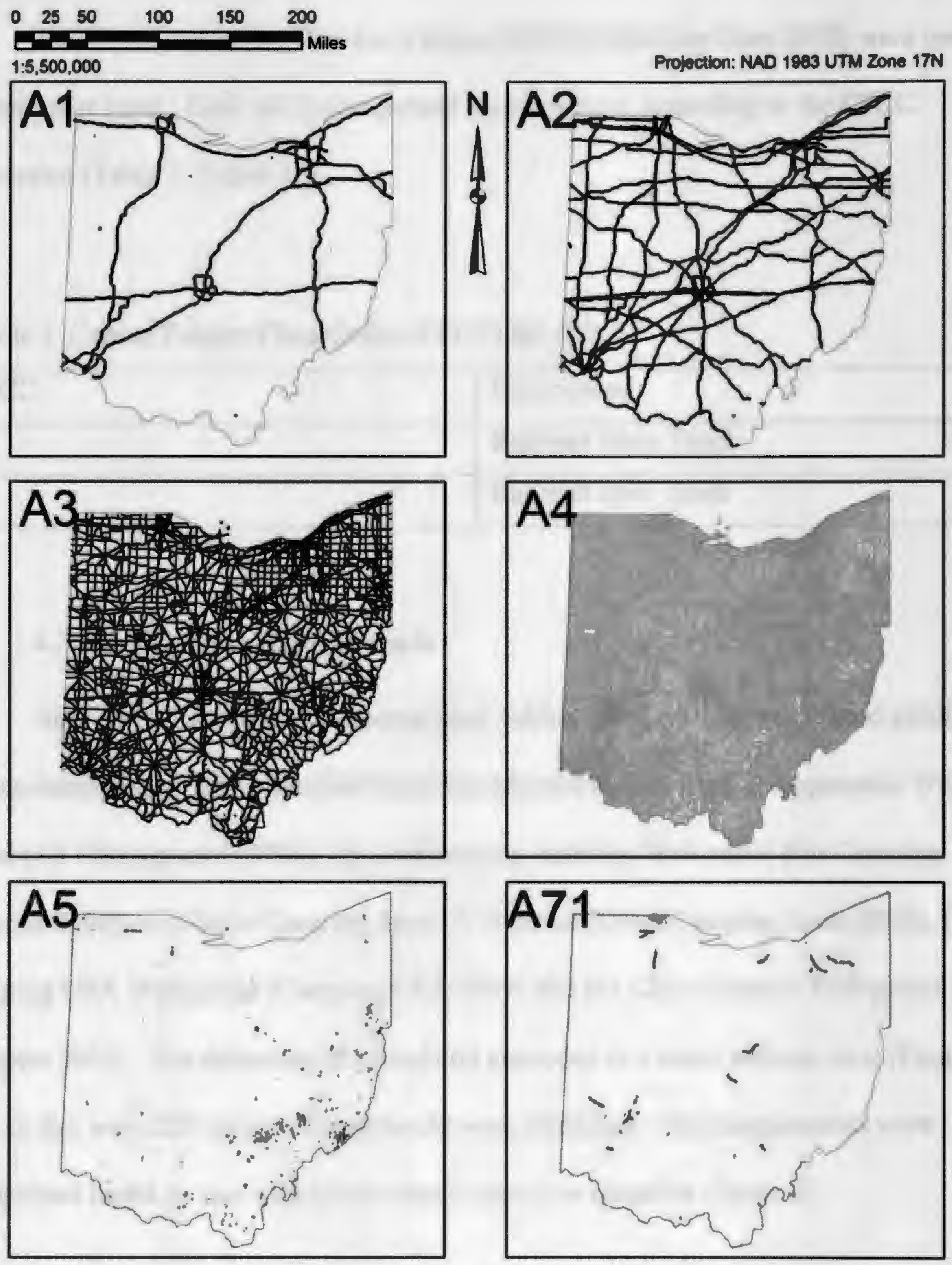

Figure 14. Ohio TIGER road centerlines by CFCC type (Data from Census 2000 TIGER/Line Data 2000)

4.2.3. Exposure to Rails

TIGER rail centerline files for (Census 2000 TIGER/Line Data 2000) were used as rail transport input. Each rail is categorized based on type, according to the CFCC description (Table 5, Figure 15).

Table 5. Census Feature Class Codes (CFCC) for rails

CFCC	Description
B1	Railroad Main Track
B2	Railroad Spur Track

4.2.4. Exposure to Campgrounds

Addresses and numbers of recreational vehicle (RV) sites for each listed public and private campground were identified from five Internet sites: (i) All Campgrounds Web portal (All Campgrounds 2008), (ii) Go Camping America Web portal (Go Camping America 2009), (iii) Great Camping Spots Web portal (Great Camping Spots 2010), (iv) Camping USA Web portal (Camping USA 2009) and (v) Ohio Campers Web portal (Ohio Campers 2010). The data were tabulated and geocoded to a street address level (Figure 16). In this way, 229 unique campgrounds were identified. The campgrounds were categorized based on size with breaks based upon five quantiles (Table 6).

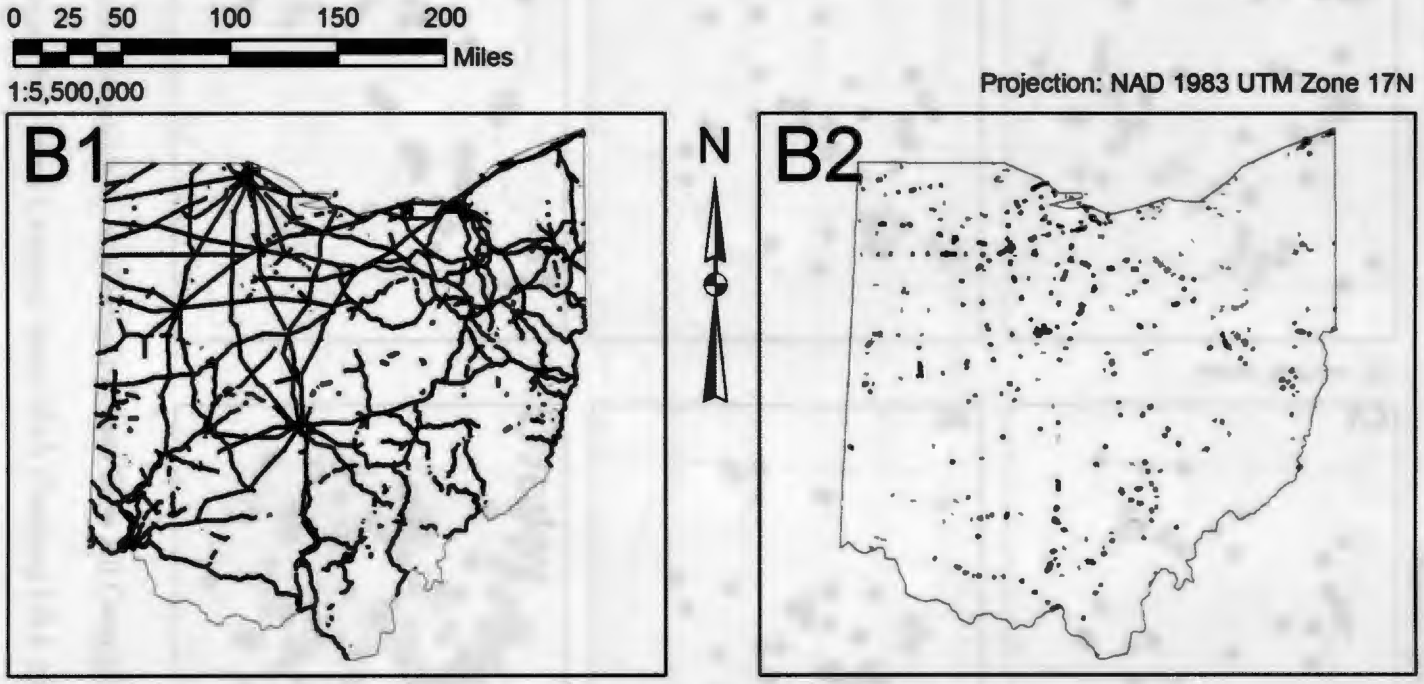

Figure 15. Ohio TIGER rail centerlines by CFCC type (Data from Census 2000 TIGER/Line Data 2000)

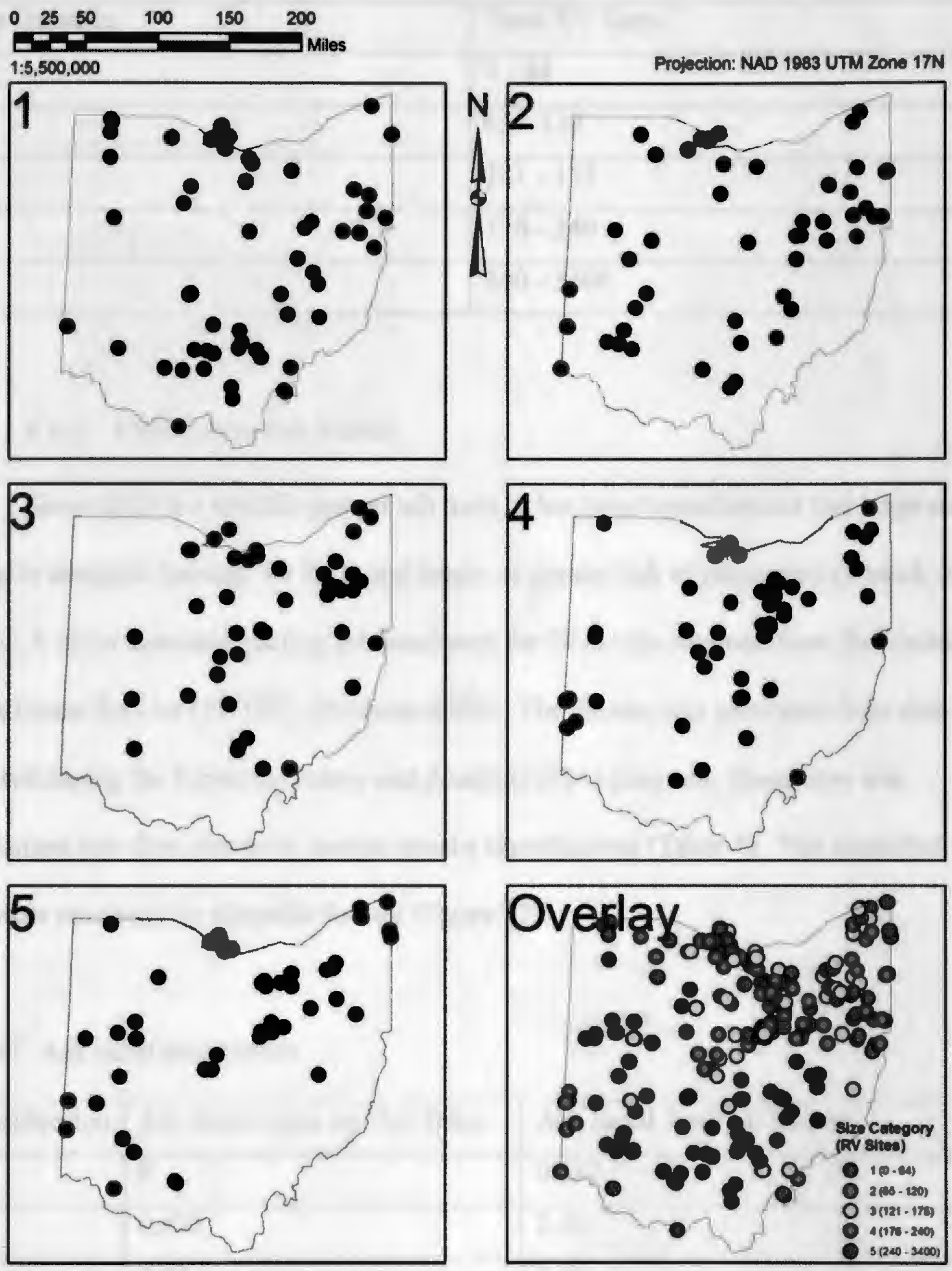

Figure 16. Ohio campgrounds by size category (Data from All Campgrounds 2008, Go Camping America 2009, Great Camping Spots 2010, Camping USA 2009 and Ohio Campers 2010)

Table 6. Campground size classes

Size Quantile	Total RV Sites
1	0 - 64
2	65 - 120
3	121 - 175
4	176 - 240
5	240 - 3400

4.2.5. Exposure to Ash Stands

Since EAB is a specific pest of ash trees, it has been hypothesized that large stands are more desirable habitats for EAB and hence, at greater risk of infestation (Prasad, *et al.* 2010). A raster dataset depicting ash basal area for Ohio was obtained from the United States Forest Service (FHTET - Products 2007). The dataset was generated from data gathered during the Forest Inventory and Analysis (FIA) program. Basal area was categorized into five classes by natural breaks classification (Table 7). The classified raster data were converted to shapefile format (Figure 17).

Table 7. Ash basal area classes

Classification	Ash Basal Area (m^2/ha) from:	Ash Basal Area (m^2/ha) to:
1	0	0.632
2	0.632	2.53
3	2.53	5.90
4	5.90	11.6
5	11.6	54.0

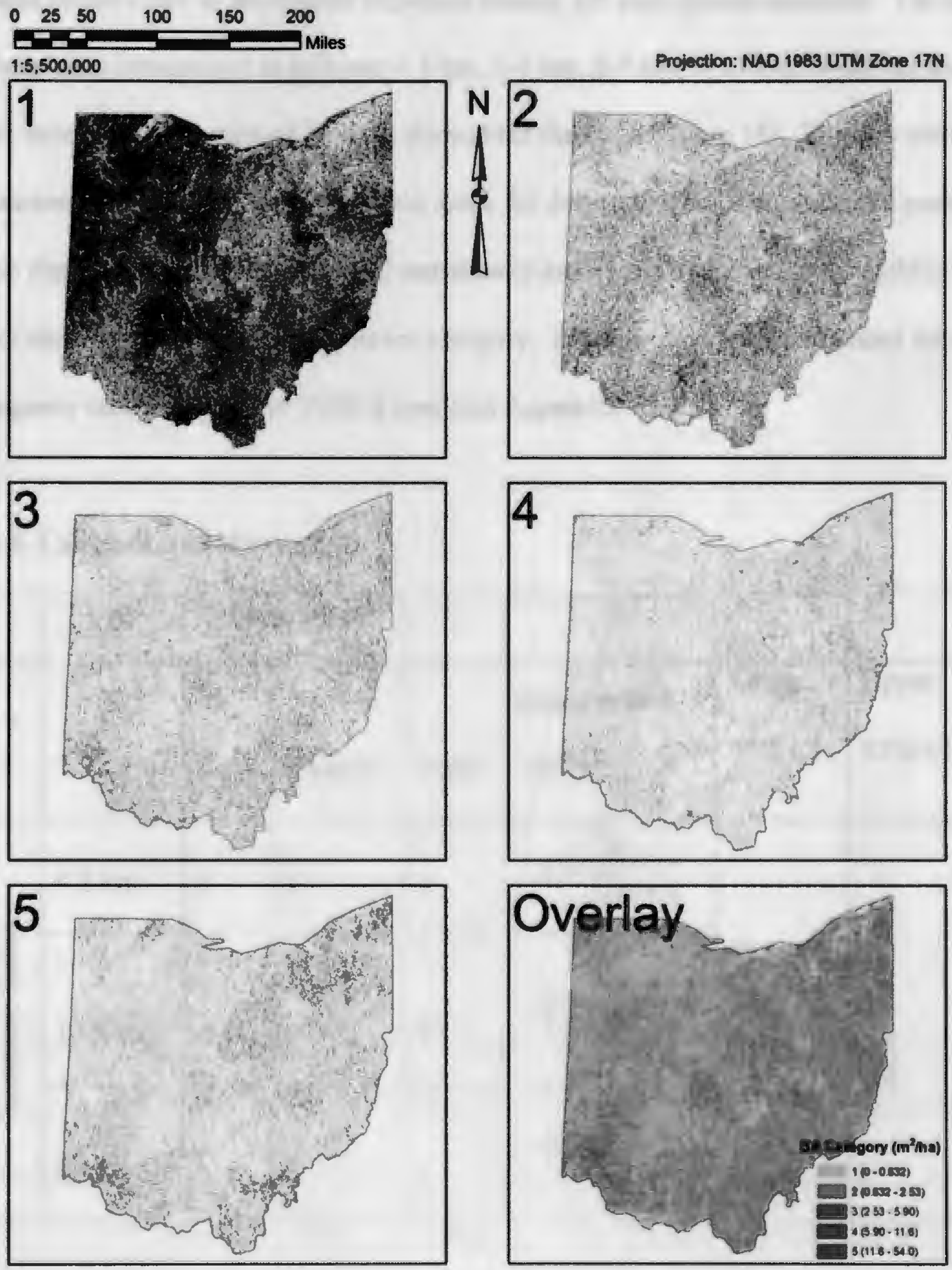

Figure 17. Ohio ash basal area classification (Data from Service (FHTET - Products 2007)

4.2.6. Generation of Relative Risks

The ArcGIS® Near tool was used to calculate the distance from each 'detection tree' and positive tree to the nearest exposure feature, for each dataset analyzed. The near distances were categorized as follows: < 1 km, 1-2 km, 2-5 km, 5-10 km, 10-20 km and > 20 km, based on the density of features throughout the state (Figure 18). Records were summarized by distance category to yield totals for detection trees and confirmed positives in each distance category. Totals were statistically analyzed using contingency tables for each of the exposure feature and distance category. Relative risks were calculated for each contingency table as shown in Table 8 (see also Appendix C).

Table 8. Calculation of relative risks

		Disease Status					
		Case	Control	Total	Relative Risk (RR)	Lower 95% CI	Upper 95% CI
Exposure Status	< 1 km	a	b	c	$\frac{a/c}{s-a/u-c}$	$RR.e^{-1.96\sqrt{SE}}$	$RR.e^{1.96\sqrt{SE}}$
	1 - 2 km	d	e	f	$\frac{d/f}{s-d/u-f}$		
	2 - 5 km	g	h	i	$\frac{g/i}{s-g/u-i}$		

Table 8. (continued)

		Disease Status					
		Case	Control	Total	Relative Risk (RR)	Lower 95% CI	Upper 95% CI
Exposure Status	5 - 10 km	j	k	l	$\frac{j/l}{s-j/u-l}$	$RR.e^{-1.96\sqrt{SE}}$	$RR.e^{1.96\sqrt{SE}}$
	10 - 20 km	m	n	o	$\frac{m/o}{s-m/u-o}$		
	> 20 km	p	q	r	$\frac{p/r}{s-p/u-r}$		
	Totals	s	t	u			

CI = Confidence Interval

4.3. Results and Discussion

4.3.1. Roads

Figure 19 shows that the features associated with the highest relative risk were A71 roads (walkways and trails for pedestrians). This result is potentially significant because other risk models (MDA 2006) and (Prasad, *et al.* 2010) do not use proximity to trails as a risk factor for EAB introduction. Unlike most other exposure features and distance categories

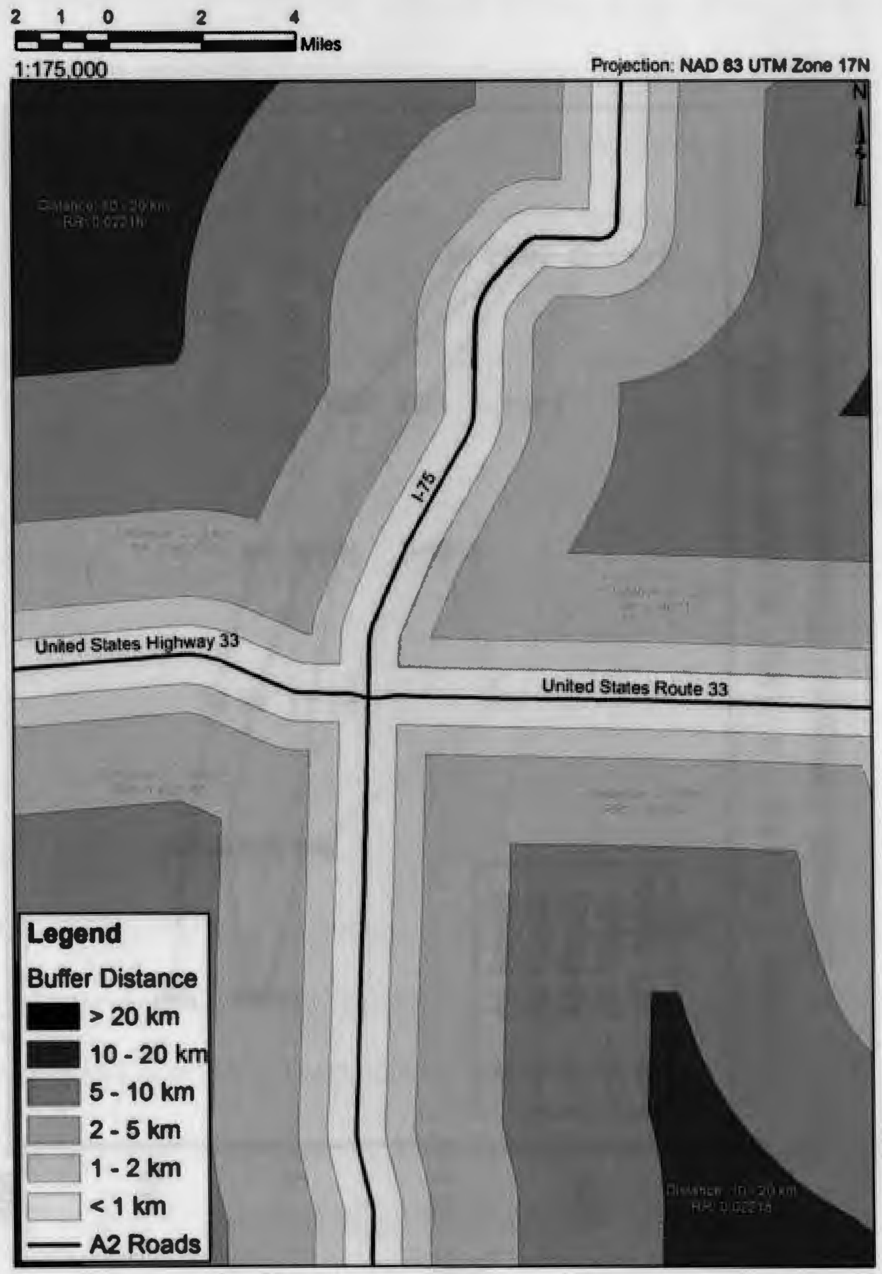

Figure 18. Example of buffers around a portion of A2 roads and the relative risks associated with each area (Data from Census 2000 TIGER/Line Data 2000)

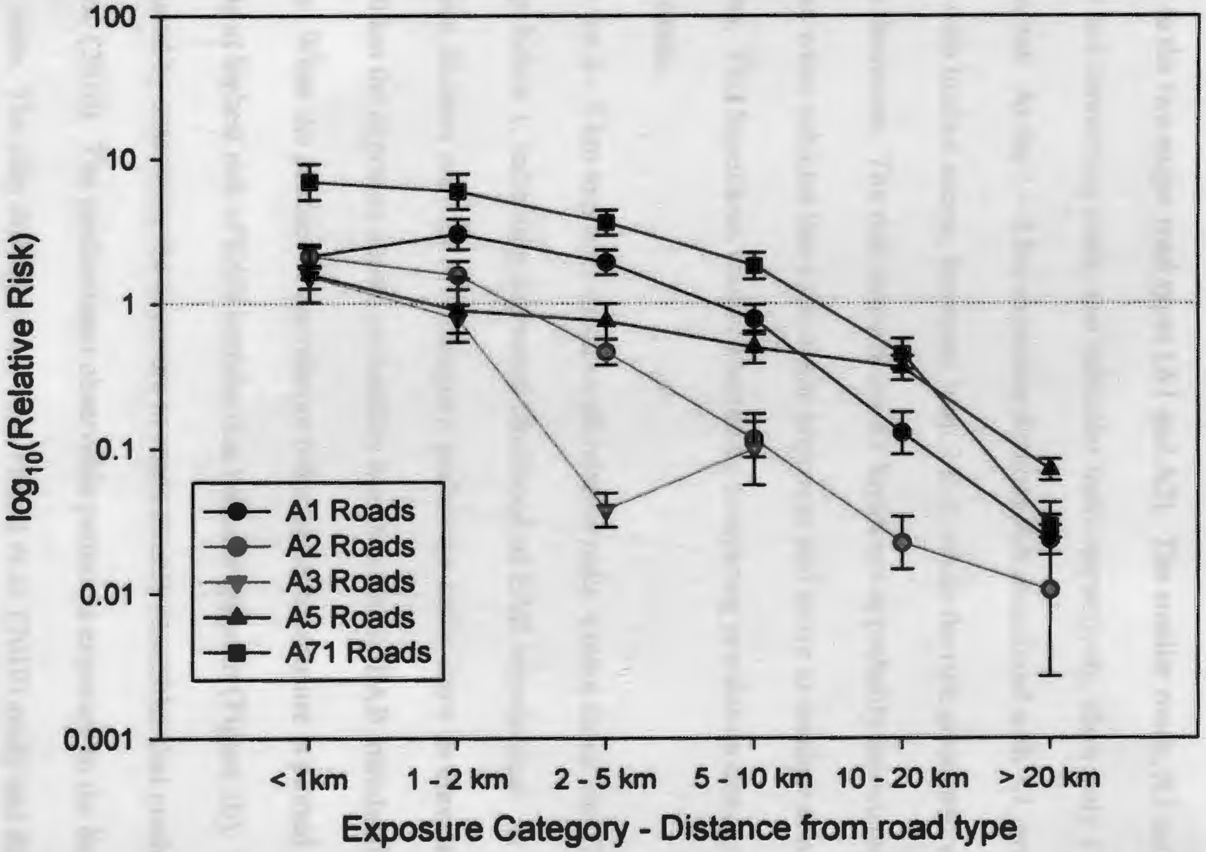

Figure 19. Relative risks for exposure to roads

examined, the relative risk of A71 roads stays above 1 through the 5 – 10 km buffer distance. This suggests that the causal factor associated with this elevated relative risk is not the roads themselves, but something highly correlated yet at a distance of up to 10 km.

At the < 1 km exposure distance there is an approximately two-fold risk for proximity to the two major road types (A1 and A2). The smaller roads, A3 and A5, secondary and connecting roads, and vehicular trails respectively, show only 1.2 – 1.5 fold increase in risk. At the 1 – 2 km exposure distance risk associated with A1, primary highways with limited access, increases from 2 to 3, while the risk associated with other road types decreases. The risk increase for A1 highways is probably associated with higher populations when vehicles leave the major highways and move to residences or other destinations. This hypothesis could be tested by comparing population density distribution to the A1 roads.

At the 2 – 5 km exposure distance all relative risks, except those for A71 and A1 roads drops below 1, indicating decreased likelihood of EAB introduction. At the 5 – 10 km exposure distance only the A71 category, pedestrian trails, show an elevated risk. Beyond 10 km the exposure shows probability less than one of EAB introduction for all road types. When the product of the relative risks for each exposure is plotted on a map of Ohio, areas at highest risk of EAB introduction become apparent (Figure 20). The risk map produced by examining the exposure to roads closely resembles that produced by Prasad *et al.* (2010). The predominant observable pattern is exposure to the large highways across the state. The only difference between Prasad *et al.* (2010) study and this one is that this study identifies high risk areas in the southeast portion of the state. This exclusion in

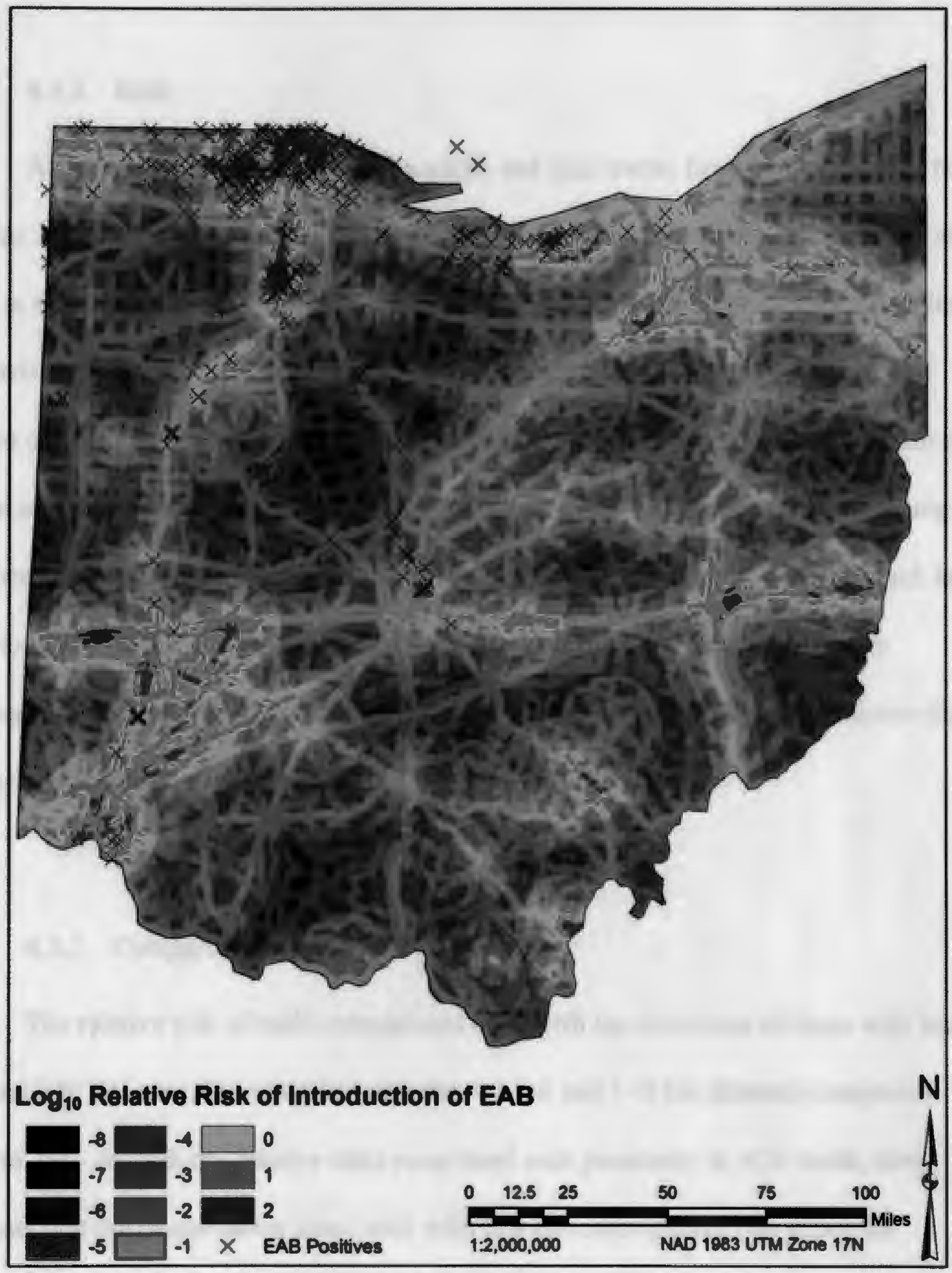

Figure 20. Ohio EAB risk due to exposure to roads

Prasad *et al.* (2010) study may be due to their utilizing an average daily traffic to derive associated weights.

4.3.2. Rails

At less than two kilometers main tracks and spur tracks have similar relative risks (Figure 21). At 2 – 5 km the relative risks associated with main tracks falls below 1 and there is a decreased probability of EAB introduction compared to spur tracks. This finding is consistent with the hypothesis that EAB introduction occurs where trains load and unload cargo. The relative risk associated with main tracks is lowest between 10 km and 20 km and is similar to the relative risk of A2 major roads. At 10 – 20 km, increasing the distance from spur tracks decreases risk of EAB introduction just one tenth as much as it does for main tracks. There are no EAB positive trees found greater than twenty kilometers from either rail type. Figure 22 depicts the sum of the log of the relative risks for each exposure due to rail transport.

4.3.3. Campgrounds

The relative risk of each campground size, with the exception of those with between 176 and 240 RV sites, increases between the < 1 km and 1 -2 km distance categories (Figure 23). As with the relative risks associated with proximity to A71 roads, this suggests that the causal factor associated with this elevated relative risk is not the campgrounds themselves, but something else as in the case of the A71 roads. Compared to other exposure scenarios, distance from campgrounds shows little decrease in relative risk.

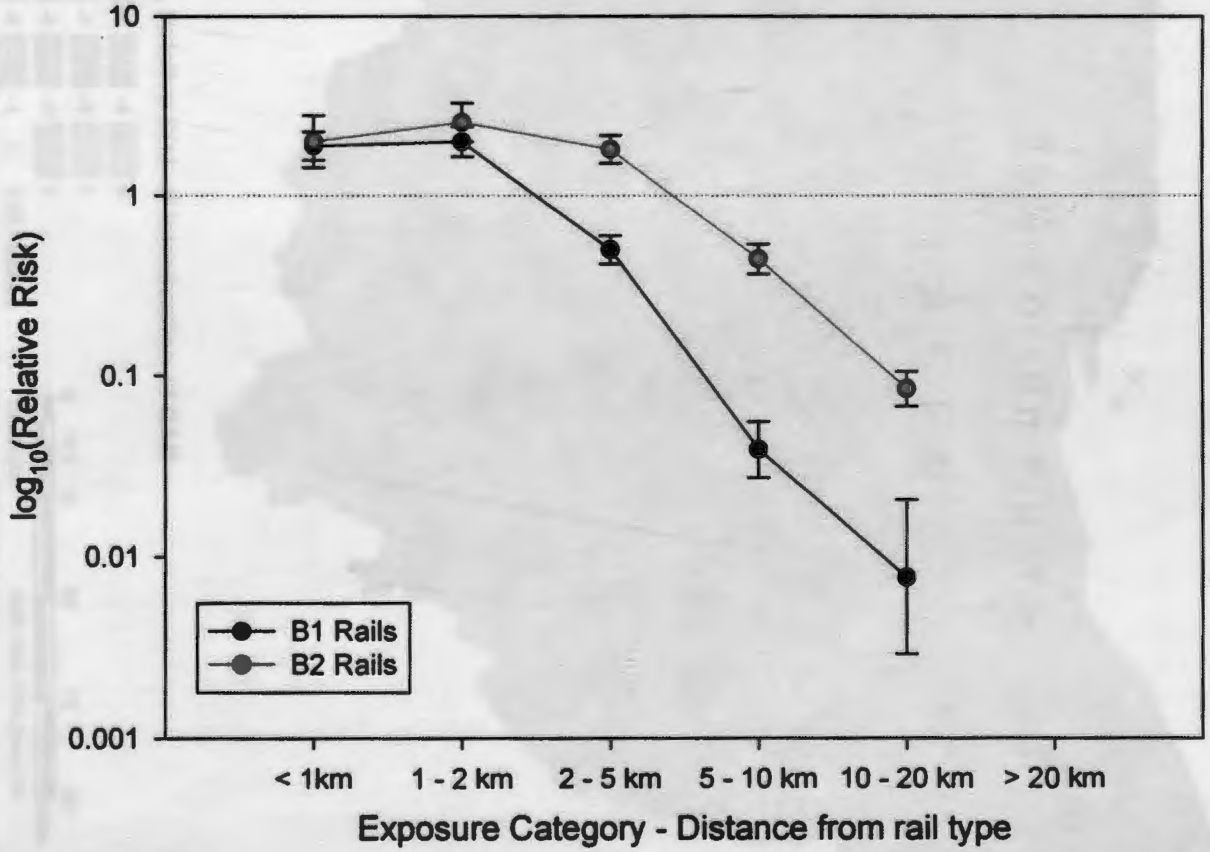

Figure 21. Relative risks for exposure to rails

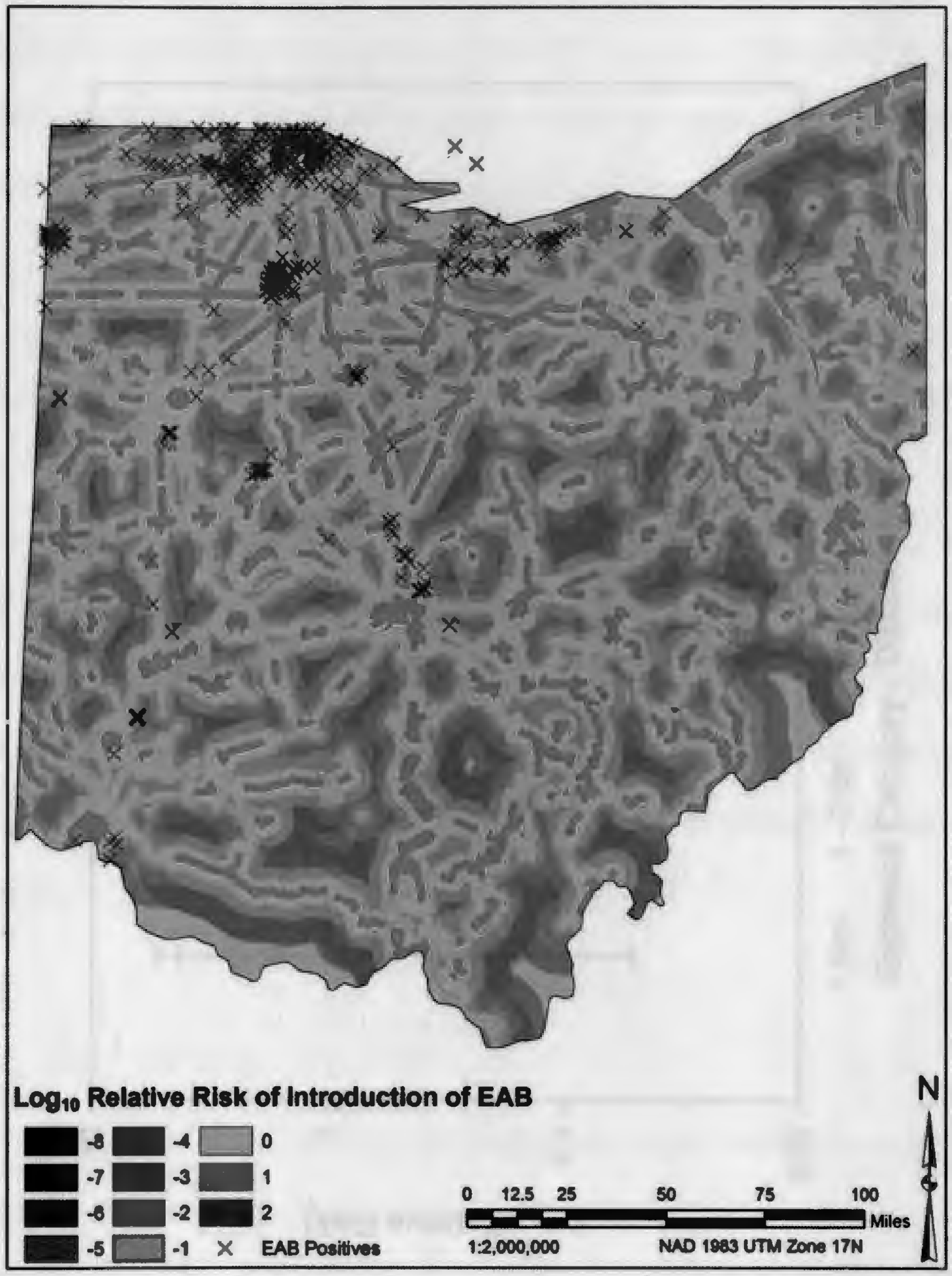

Figure 22. Ohio EAB risk due to exposure to rails

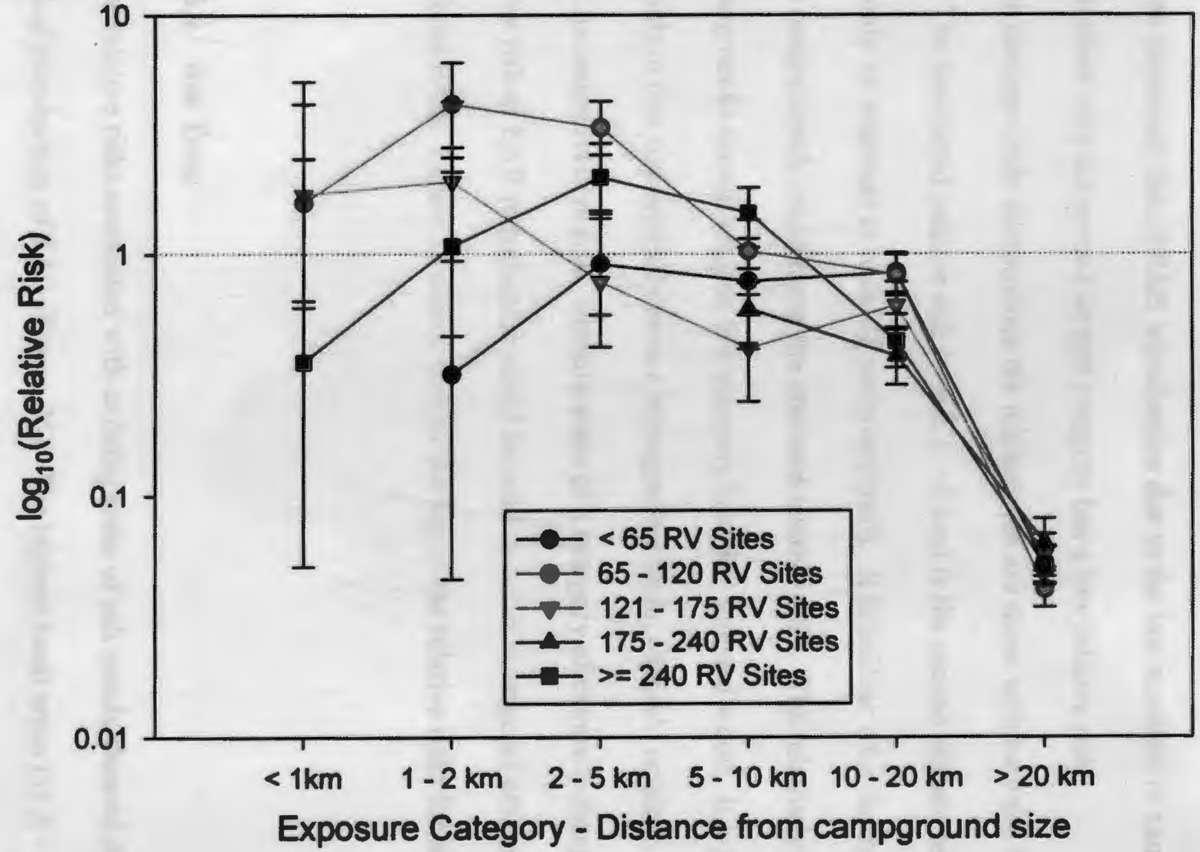

Figure 23. Relative risks for exposure to campgrounds

The trend lines stay relatively flat (relative risk > 0.1) before dipping between 10 and 20 km from the campgrounds (relative risk < 0.1). Campgrounds with less than 65 RV sites and those with between 176 and 240 RV sites are unique in that they are the only exposures measured that do not show any increased risk EAB introduction. The smallest category possibly has decreased risk of EAB introduction due to the low numbers of campers at each site. It is unclear why the second largest category has a low relative risk.

The campgrounds that produce the highest risk are those with between 65 and 120 RV sites. The associated relative risk (= 4.2, 1 – 2 km) is the second highest seen, exceeded only by exposure to walking paths and trails. It is unclear what factors associated with these campgrounds could cause the elevated relative risks. The relatively small size of the campgrounds should suggest few campers bringing infested wood. It is possible that campgrounds of this size typically have a management style, clientele or other, non-spatial, factor that increases relative risk. Identification of a category of campsite that produces a high relative risk of EAB introduction could be used to assist in targeted efforts to educate campers about EAB. Figure 24 shows sum of the log of the relative risks for each exposure.

4.3.4. Ash Trees

The relative risks associated with existing areas of ash stands showed decreased likelihood of introduction of EAB (Figure 25). The highest basal areas (11.6 – 54.0 m^2/ha) had modestly elevated risk of introduction of EAB at small distances (< 2 km), which is surprising since areas dense in ash are predicted to be hotspots in Prasad *et al.*'s (2010)

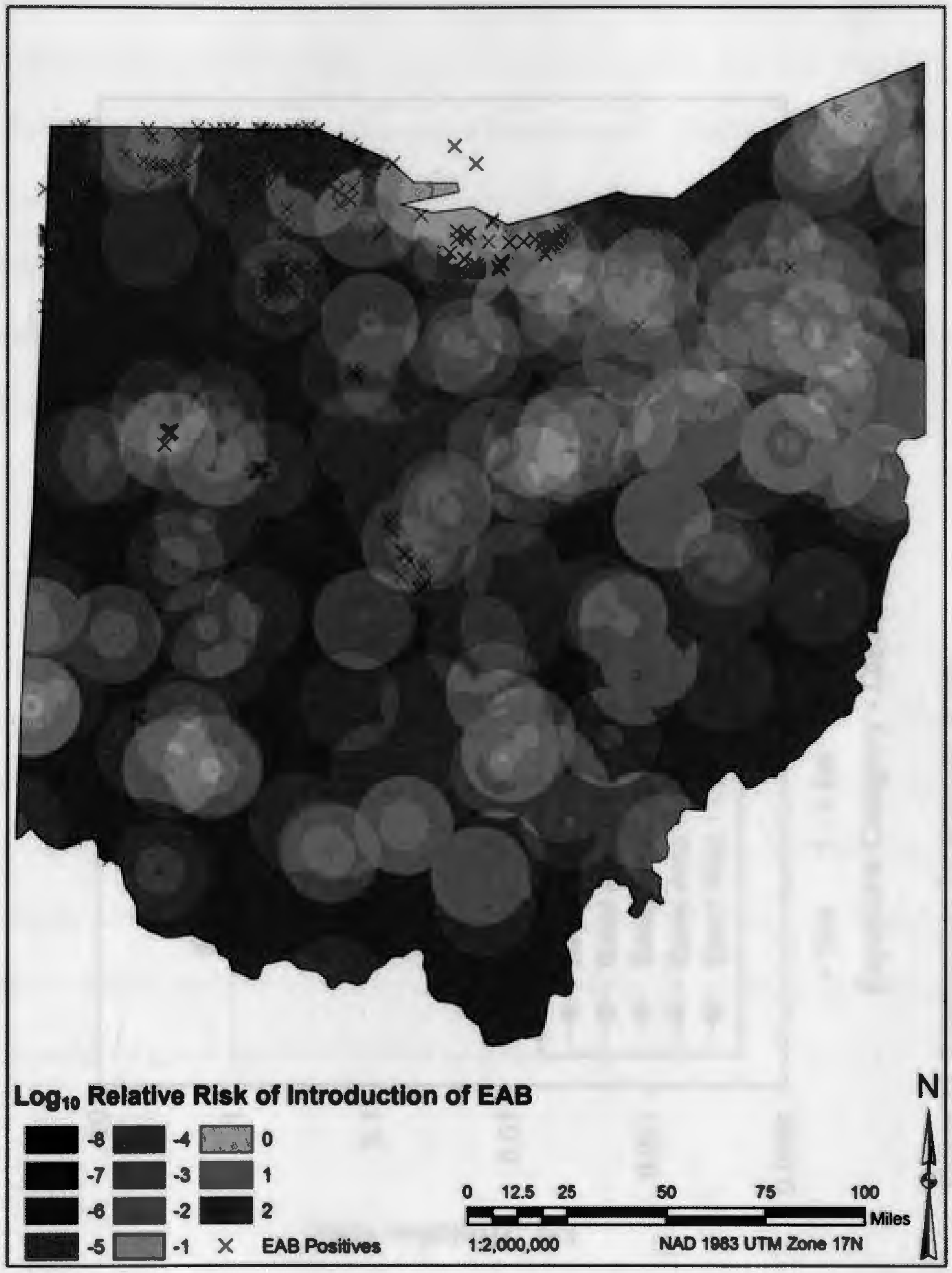

Figure 24. Ohio EAB risk due to exposure to campgrounds

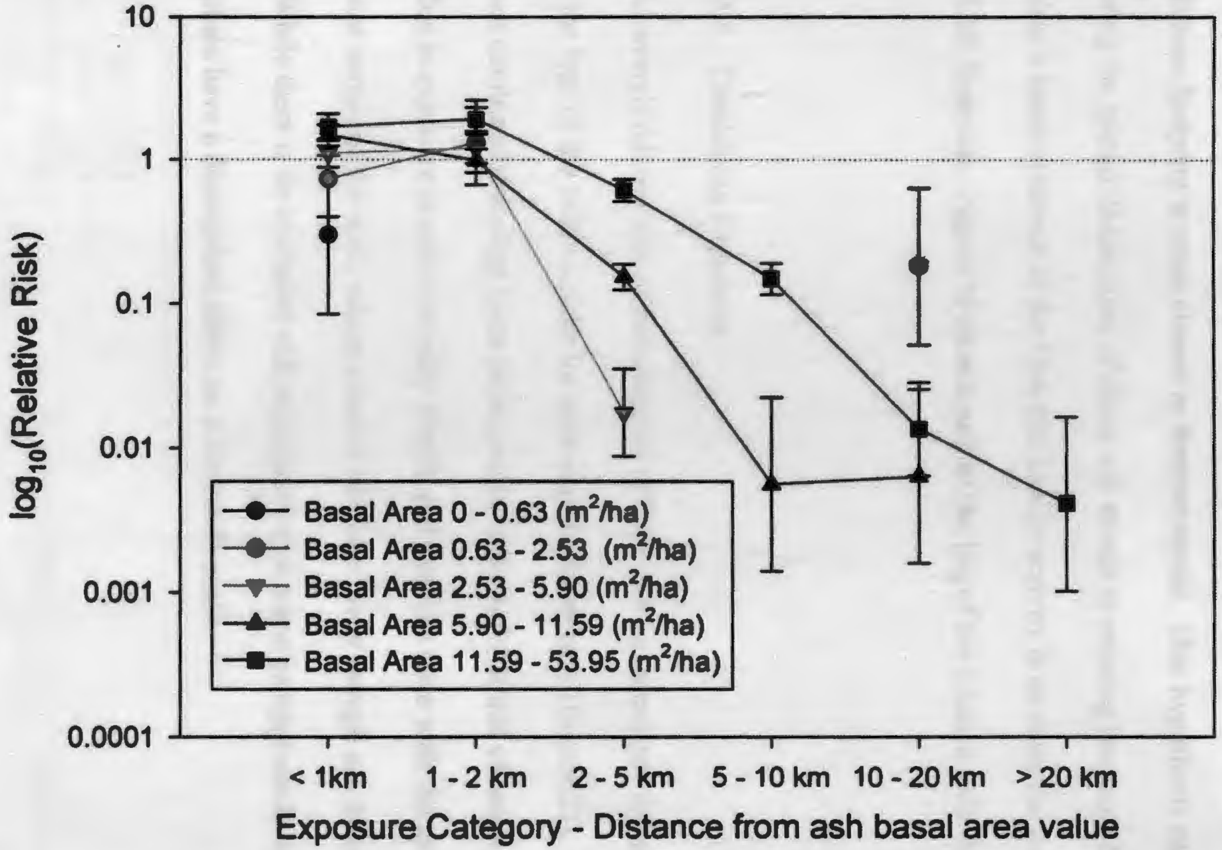

Figure 25. Relative risks for exposure to ash

gravity model. The lowest three classes have missing data points because their features are numerous and there are no EAB positives trees that fall in the larger distance categories. Further than 2 km from the three densest ash basal areas the relative risk decreases rapidly, showing the lowest relative risks seen in the analysis (< 0.01). This may be attributed to minimal human footprint at areas closest to densest stands. This hypothesis can be tested by comparing the spatial distribution of dense ash stands to existing landuse. If this can be attested, then it lends credence to the idea that human activity is an essential mode of long distance EAB dispersal. Figure 26 shows sum of the log of the relative risks for each exposure.

4.3.5. Combining Exposures

The overall relative risk of introduction of EAB can be calculated for an area by summing the logs of the relative risks for each exposure category (Figure 27). The areas with highest combined risk align most prominently with the locations of roads and rails. The risk due to exposure to ash is broadly distributed over the state with the exception of the southeast corner of the state, where relative risks are lower though ash density is highest. While there is an increased risk associated with some campgrounds the relatively small numbers have a diminished effect on a statewide scale.

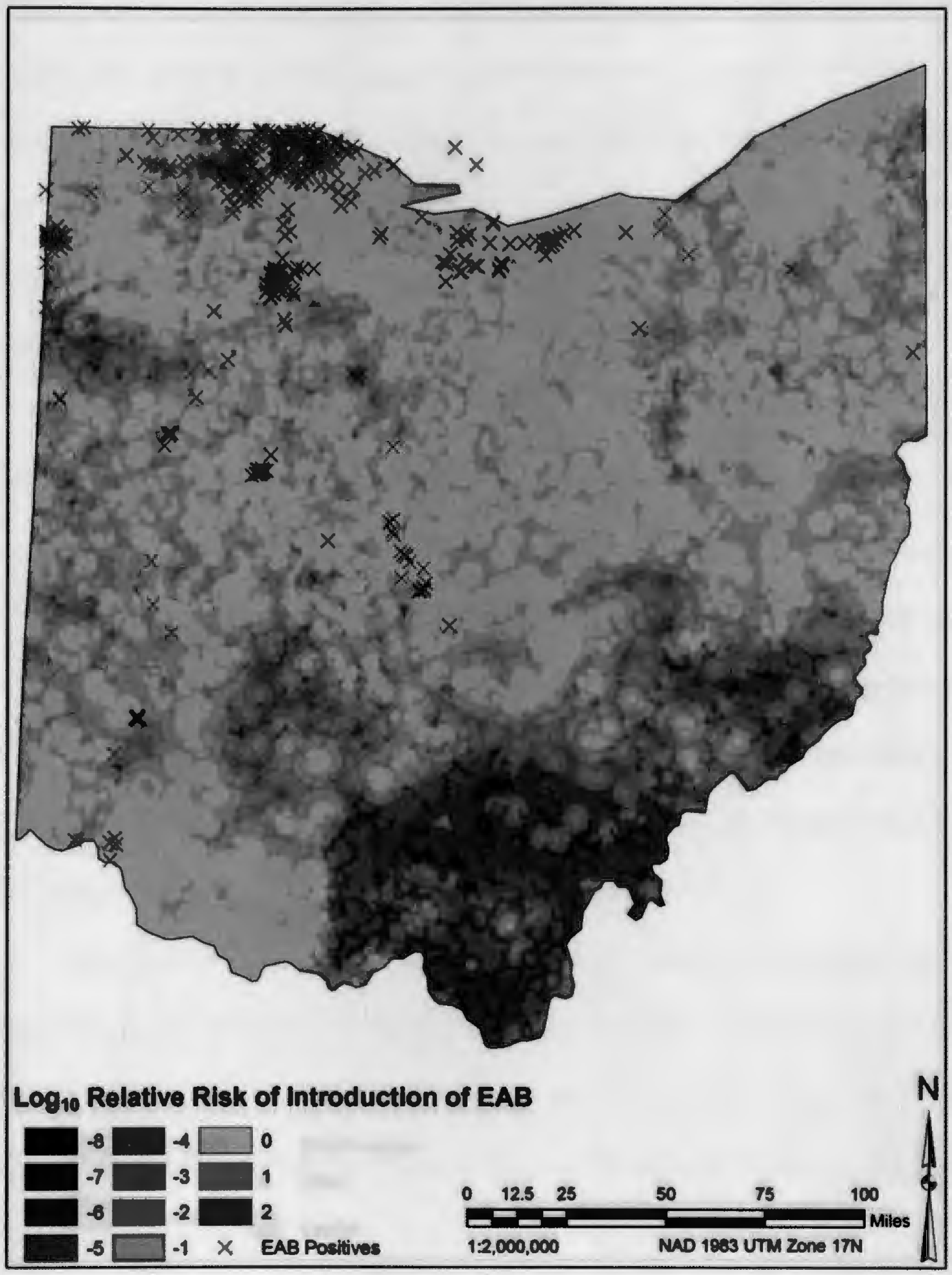

Figure 26. Ohio EAB risk due to exposure to ash

Figure 27. Ohio EAB risk due to all exposures

4.4. Model Application

Exposure features corresponding to those defined for Ohio were collected for North Dakota: roads, rails, campgrounds and ash tree locations. The relative risks calculated for each exposure type and distance category in the Ohio case, were assigned to the corresponding features to generate comparative risk values for North Dakota. Unlike Ohio, there is little high risk that can be attributed to roads for North Dakota. The high risk areas are confined to the two major metropolitan areas of Fargo and Grand Forks, where there exists a higher density of roads (Figure 28).

Exposure to rails is a large cause of the elevated relative risks across the state. North Dakota is relatively well covered by railway networks, with exceptions on large unconnected areas at Theodore Roosevelt National Park, Little Missouri National Grassland and south of Interstate 94 around the Heart Butte Reservoir Game Management Area, west of the Missouri River (Figure 29). The relative paucity of campgrounds in North Dakota implies that the risks due to campground exposure are comparably diminished. However, most of the campgrounds in North Dakota belong to the second size class, which elevates associated risk (Figure 30).

North Dakota has more isolated regions of high density ash tree stands than does Ohio. This yields a relative risk map that contains very high risk areas around the Turtle Mountains in the north central part of the state and at the Theodore Roosevelt National Park. In addition there are regions of high relative risk along the main riparian corridors (Figure 31).

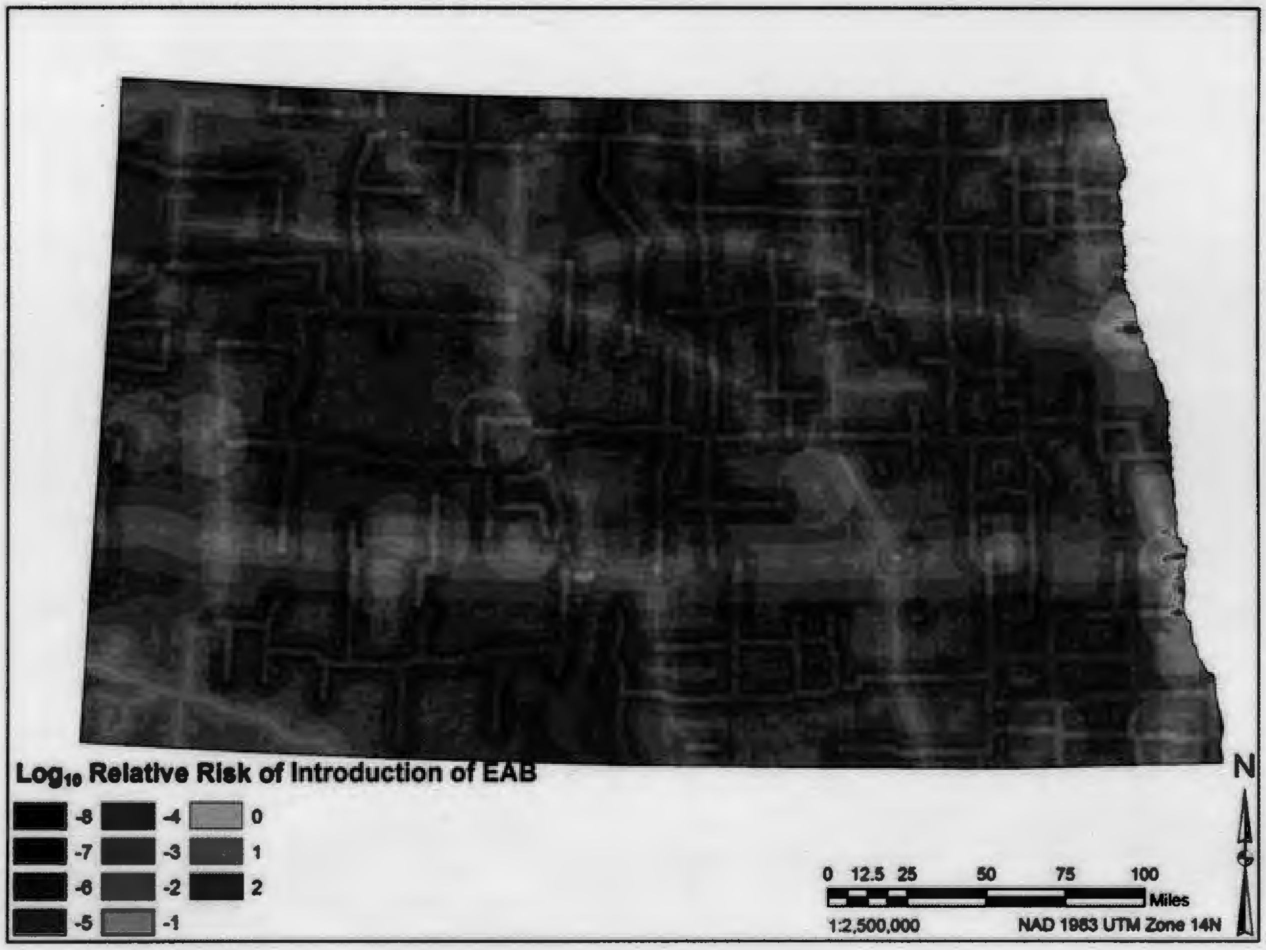

Figure 28. North Dakota EAB risk due to exposure to roads

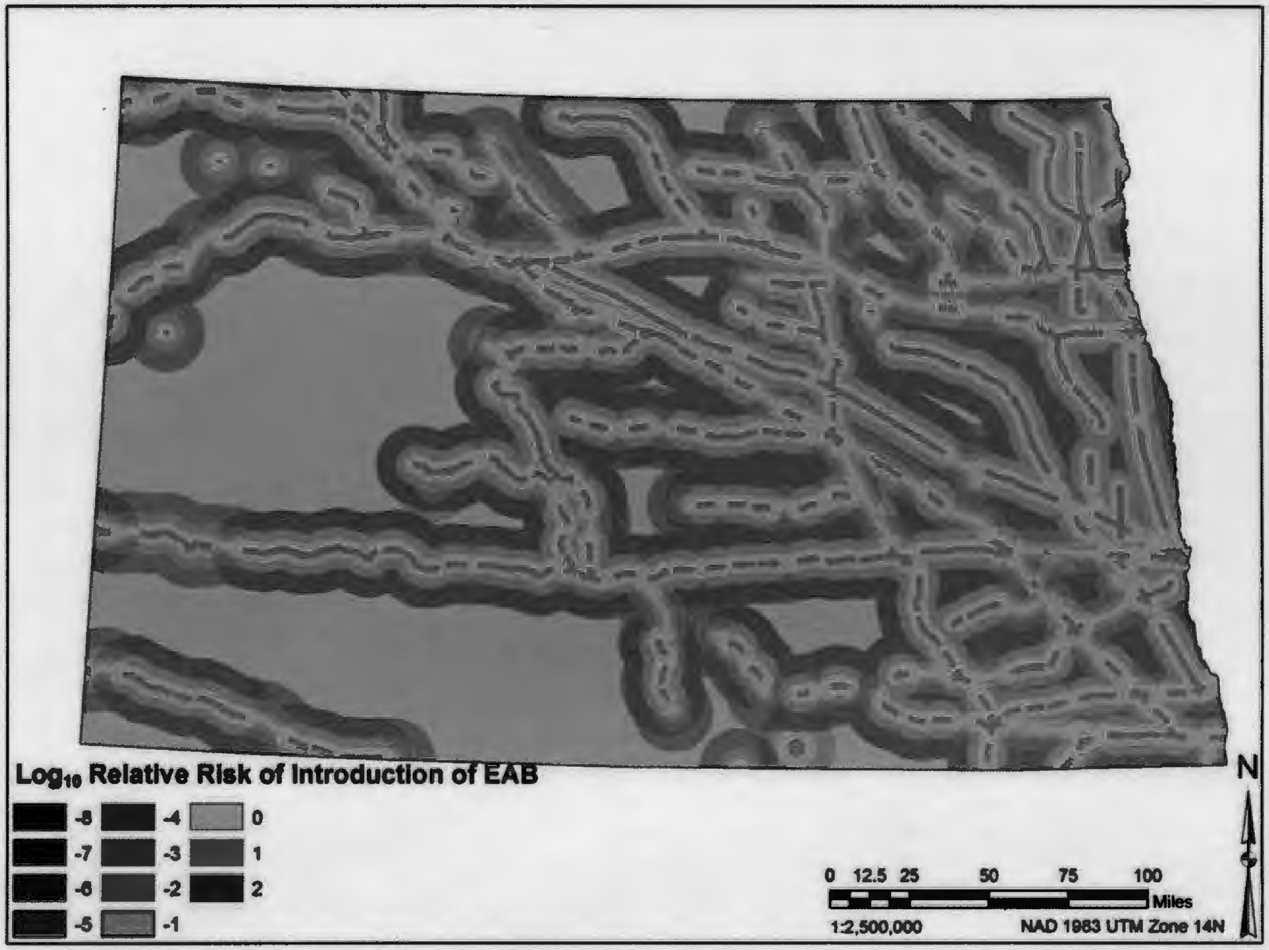

Figure 29. North Dakota EAB risk due to exposure to rails

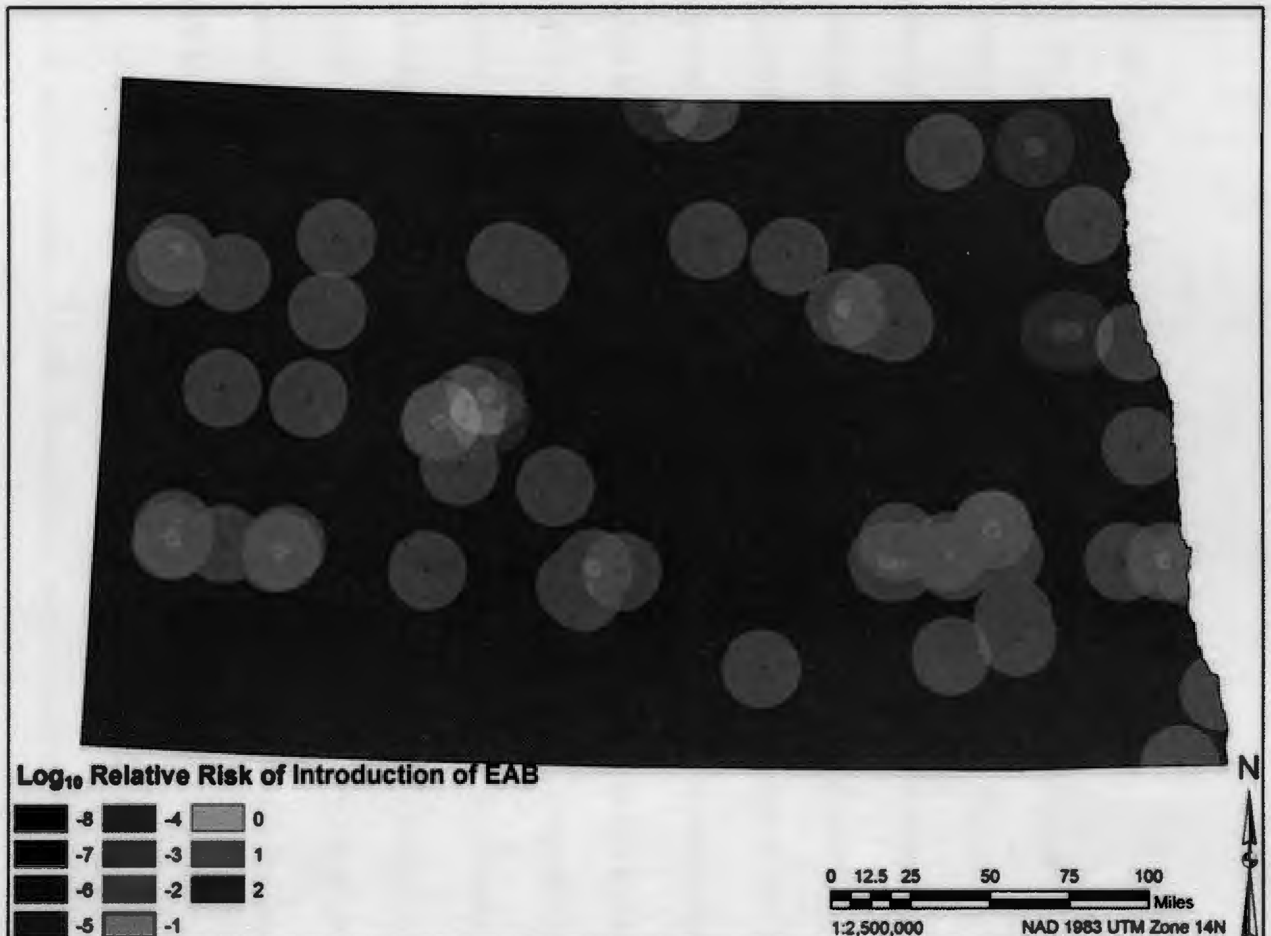

Figure 30. North Dakota EAB risk due to exposure to campgrounds

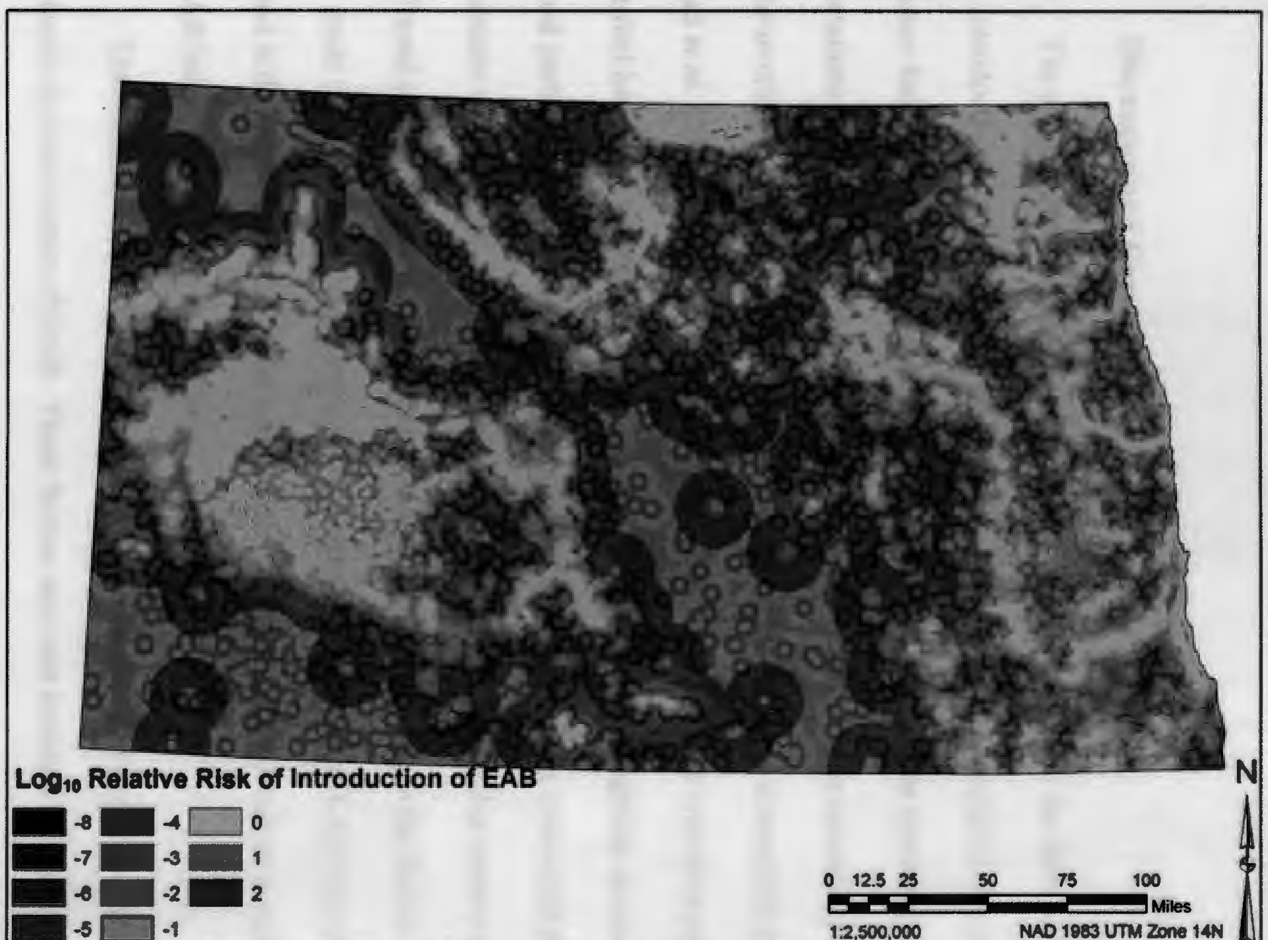

Figure 31. North Dakota EAB risk due to exposure to ash

When the log of the relative risks of the four exposure types are summed the result is a risk map that displays elevated exposure pathways in areas associated with rails and along the major river systems of North Dakota (Figure 32).

4.5. Discussion and Conclusions

The process outlined here describes a method of quantifying the risks associated with introduction of EAB. A prior study (MDA 2006) arbitrarily assigned risk values to exposure factors, then amalgamated factors according to a regression equation that matched expectations. The method highlighted in this study may be useful in cataloging areas that can be overlooked in the course of developing a statewide strategic assessment plan. Prasad *et al.* (2010) developed a detailed model though it overlooks critical exposures identified here. The method presented here allows quantitative weighting across all defined pertinent factors that may influence EAB spread to obtain a more accurate assessment of EAB risk. This approach yielded a geospatial model that closely replicates the Prasad *et al.* (2010) results, with two notable exceptions. First, is the failure to identify A71 roads (walkways and hiking trails) as an important predictor of EAB infestation. Second is the over-estimation of the importance of high densities of ash as a gravity center of EAB infestation.

The Prasad *et al.* (2010) model includes wood product industries and nurseries as a risk factor for introduction of EAB. These factors were not included in this model because, as Prasad *et al.* (2010) elucidate, there is much increased regulation of such industries after

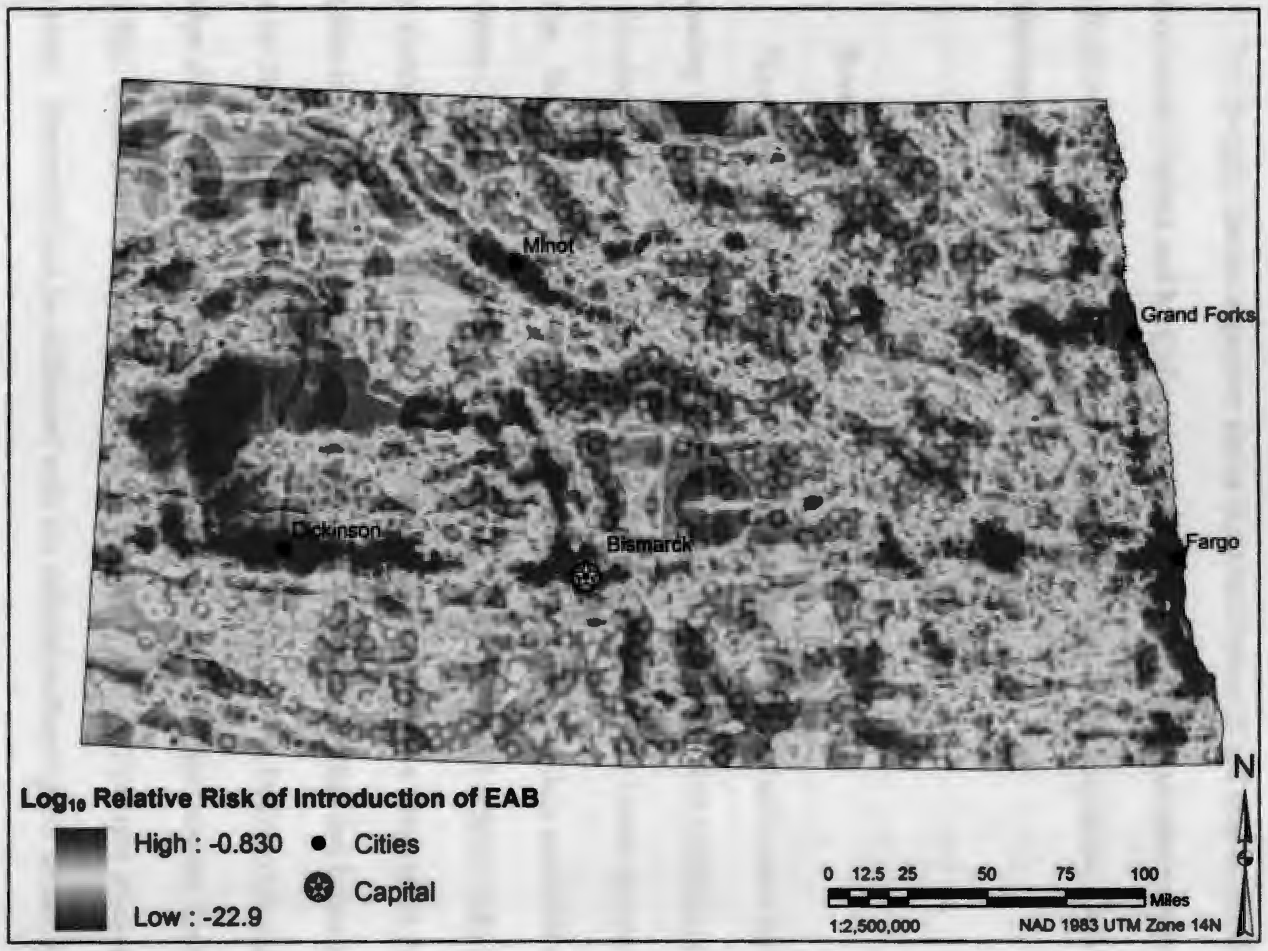

Figure 32. North Dakota EAB risk due to all exposures

the initial discoveries of EAB associated with them. Campgrounds may be subject to such regulation in the future, but present more of a regulatory challenge than nurseries, because of increased numbers of allied businesses statewide and nationwide.

It is thought that an important factor in attractiveness of ash trees to EAB is their relative health (Poland and McCollough 2006). Though an accurate assessment of tree health across a state is difficult to obtain it may provide a useful risk factor EAB introduction.

4.6. Recommendations

Prasad *et al.* (2010) validated their model by calculating relative risks for roads and comparing them to the weighting they used in their calculations. The model presented here was developed to serve primarily as a strategic assessment tool for North Dakota Forest Service. Because the model was developed using the only cohort data available at the time, data from Ohio, some assessment of the accuracy of the calculated relative risks applied to other states is required. The relative risks calculated for Ohio are a geographic proxy for the behavior of individuals who spread EAB and the assumption that that behavior is the same in Ohio and North Dakota was made in preparing the North Dakota risk map. In addition there are differences in the landscape, climate and ecology between North Dakota and Ohio, which could affect the reliability of the calculated relative risks when applied to new areas. The model can be calibrated with the defined anthropogenic spread of EAB in other states. Risk maps for states with new introductions of EAB are generated using the relative risks calculated for Ohio. The calculated risk maps would then be compared to known outbreaks of EAB. The correlation between introduction of EAB and high risk areas would allow model refinement and sensitivity analyses. With EAB already detected in much of the Midwest, effort is being put into containing the outbreak. The question for forest health partners in states adjacent to confirmed EAB locations is how this information can be used to modify current management practices and aid in quarantine demarcations. The step usually initiated by responsible agencies, the state Department of Agriculture or United States Department of Agriculture – Animal and Plant Health Inspection Service, is effective monitoring and tracking EAB. Once EAB is detected in a region, an emergency quarantine may be imposed (Minnesota Emerald Ash Borer Response Plan 2007). Risk maps can then be used to help define the area of quarantine as well as determine appropriate regulations to prevent the spread to adjacent areas. Two protocols, 'detection trees' and EAB traps (Emerald Ash Borer Surveys 2011) are largely being used. Risk maps such as the ones produced here are useful aids to guide the placement of such indicators.

CHAPTER 5.SUMMARY

The over-arching goal of this study is to offer insight on high risk areas for EAB establishment that can be used to develop the management strategies available in the face of EAB spread across the Midwest, toward North Dakota. To this end the study has generated a spectral library of common North Dakota forest trees that describes the variation to be seen among the common genera. In addition an analysis of the potential useful orbital platform that may offer optimal information for rapid ash tree identification is discussed, but not validated. The study also develops and utilizes a geospatial model to estimate risk of EAB introduction to North Dakota. The results of the risk model show areas of North Dakota that would likely display exposure pathways to an EAB introduction. The risk model can be used as a baseline guide to respective federal agencies as they monitor and or in the event of EAB introduction to mitigate an EAB threat.

REFERENCES

Alberman, E D, Butler, N R and Sheridan M D. "Visual acuity of a national sample (1958 Cohort) at 7 years." *Developmental Medicine and Child Neurology*, 1971: 13(1) : 9 -14.

All Campgrounds. 2008. http://www.allcampgrounds.com (accessed October 2010).

Ayersman, W, Strager, M and Strager, J. "Modeling Emerald Ash Borer Establishment and Spread Using GIS." *2009 ESRI Users Conference.* San Diego: ESRI, 2009.

BenDor, T K, Metcalf, S S, Fontenot, L E, Sangunnett, B and Hannon, B. "Modeling the spread of the Emerald Ash Borer." *Ecological Modelling*, 2006: 197: 221–236.

Camping USA. 2009. http://www.camping-usa.com (accessed November 2010).

"Census 2000 TIGER/Line Data." *ESRI Free Data.* 2000. http://www.esri.com/data/download/census2000-tigerline/index.html (accessed October 2010).

"Emerald Ash Borer Surveys." *Winconsin Department of Natural Resources.* http://dnr.wi.gov/forestry/fh/ash/eab-surveys.htm (accessed March 2011).

Earth Observing 1 (EO-1). 2010. http://edcsns17.cr.usgs.gov/eo1/ (accessed March 2011).

Emerald Ash Borer. 2010. http://emeraldashborer.info/ (accessed May 7, 2010).

"FHTET - Products." *Forest Health Technology Enterprise Team Web site.* 2007. http://www.fs.fed.us/foresthealth/technology/nidrm.shtml (accessed June 2010).

Go Camping America. 2009. http://gocampingamerica.com/index.aspx (accessed October 2010).

Great Camping Spots. 2010. http://greatcampingspots.com/Directory/Index.asp?Current=Welcome (accessed October 2010).

Haugen, D E, Kangas, M, Crocker, S J, Perry, C H, Woodall, C W, Butler, B J, Wilson, B T and Kaisershot, D J. *North Dakota's Forests.* Newtown Square: USDA Forest Service, 2005.

Herman, D E and Chapu, L J. *Trees and Shrubs of North Dakota.* Fargo: NDSU Extension Services, 2003.

Herms, D A, McCullough, D G and Smitley, D R. "Under Attack." *American Nurseryman,* 2004: October: 20-26.

Landsat Handbook. 2008. http://landsathandbook.gsfc.nasa.gov/handbook/handbook_htmls/chapter5/chapter5.html#Menu (accessed March 2011).

Lerner, D J and Kannel, W B. "Patterns of coronary heart disease morbidity and mortality in the sexes: A 26-year follow-up of the Framingham population." *American Heart Journal,* 1986: 111(2): 383-390.

LP DAAC. 2011. *Land Processes Distributed Active Archive Center.* https://lpdaac.usgs.gov/ (accessed March 2011).

Minnesota Department of Agriculture. "Emerald Ash Borer Introduction Risk Model for Minnesota." 2006.

Minnesota Department of Agriculture. *News Release.* May 14, 2009. http://www.mda.state.mn.us/news/releases/2009/nr-2009-05-14-eab.aspx (accessed May 10, 2010).

Minnesota Department of Agriculture. "Minnesota Emerald Ash Borer Response Plan." 2007.

Muirhead, J R, Leung, B, van Overdijk, C, Kelly, D W, Nandakumar, K, Marchant, K R and MacIsaac, H J. "Modelling local and long-distance dispersal of invasive emerald ash borer Agrilus planipennis (Coleoptera) in North America." *Diversity and Distributions*, 2006: 12: 71 - 79.

Ohio Campers. 2010. http://ohiocampers.com (accessed October 2010).

Poland, T M and McCollough, D G. "Emerald ash borer: invasion of the urban forest and the threat to North America's ash resource." *Journal of Forestry*, 2006: 104: 118–124.

Prasad, A M, Iverson, L R, Peters, M P, Bossenbroek, J M, Matthews, S N, Sydnor, T D and Schwartz, M W. "Modeling the invasive emerald ash borer risk of spread using a spatially explicit cellular model." *Landscape Ecology*, 2010: 25: 353-369.

"Public Law 110 - 234 - Food, Conservation, and Energy Act of 2008." *US Government Printing Office.* 2008. http://www.gpo.gov/fdsys/pkg/PLAW-110publ234/content-detail.html (accessed March 2011).

Research Systems, Inc. *ENVI User's Guide.* Boulder, CO: Research Systems, Inc., 2003.

Scott, J M. "How to Conduct a Gap Analysis." Vers. 2.0.1. *GAP.* USGS, National Biological Information Infrastructure. 2007. ftp://ftp.gap.uidaho.edu/products/handbookpdf/CompleteHandbook.pdf.

Sydnor, T D, Bumgardner, N and Todd, A. "The potential economic impacts of emerald ash borer (*Agrilus planipennis*) on Ohio, US communities." *Arboric Urban Forestry*, 2007: 33(1): 48–54.

Woodall, Christopher W, Conkling, B L, Amacher, M C, Coulston, J W, Jovan, S, Perry, C H, Schulz, B, Smith, G C and Will-Wolf, S. *The Forest Inventory and Analysis Database Version 4.0: Database Description and Users Manual for Phase 3.* General Technical Report, Newtown Square: United States Forest Service, 2009.

APPENDIX A. SPECTRAL LIBRARY COMPOSITION

Genus	Species (Profile Count)	Cultivar (Profile Count)
Acer	A. ginnala (24)	
	A. negundo (48)	
	A. platanoides (26)	
	A. saccharinum (23)	
	A. x freemanii (2)	
Aesculus	A. glabra (2)	
Amelanchier	A. alnifolia	'Martin' (1)
		'Northline' (1)
Betula	B. lenta (11)	
	B. papyrifera (25)	
Caragana	C. arborescens (10)	
Celtis	C. occidentalis (27)	
Cornus	C. sericea (2)	
Elaeagnus	E. angustifolia (24)	
Fraxinus	F. americana (21)	
	F. mandshurica (19)	
	F. nigra (43)	
	F. pennsylvanica (56)	
	F. pennsylvanica	'Western Dakota' (24)

Gleditsia	G. triacanthos (16)	
Hippophae	H. rhamoides (11)	
Juglans	J. nigra (28)	
Juniperus	J. scopulorum (26)	
	J. virginiana (11)	
Larix	L. sibirica (12)	
Lonicera	L. edulis	'Borealis' (1)
Maackia	M. amurensis (2)	
Malus	*sp.* Unknown (16)	
Picea	P. glauca var. densata (25)	
	P. meyeri (13)	
	P. pungens (15)	
Pinus	P. banksiana (11)	
	P. cembra (12)	
	P. flexilis (11)	
	P. ponderosa (12)	
	P. resinosa (12)	
	P. sylvestris (12)	
Populus	P. deltoids (15)	
	P. tremuloides (24)	
	P. x euramericana (8)	

	P. x canadensis (25)	
Prunus	P. americana (2)	
	P. avium (2)	
	P. maackii (3)	
	P. padus (2)	
	P. serotina (3)	
	P. virginiana (27)	
	P. virginiana	'Schubert' (2)
Quercus	Q. macrocarpa (29)	
Rhus	R. glabra (2)	
Robinia	R. pseudoacacia (2)	
Salix	S. alba (17)	
	S. alba	'Vitellina' (8)
Shepherdia	S. argentea (13)	
Syringa	S. pekinensis (2)	
	S. prestoniae (2)	
	S. reticulate (2)	
	S. vulgaris (10)	
	S. vulgaris	'Katherine Havermeyer' (2)
Tilia	T. americana (38)	
	T. cordata (25)	

	T. mongolica (2)	
Ulmus	U. americana (21)	
	U. pumila (11)	
29	59	7

APPENDIX B. TRAINING DATA

File	Northern Extent (Degrees)	Southern Extent (Degrees)	Eastern Extent (Degrees)	Western Extent (Degrees)	Centroid (Longitude/Latitude Degrees)
Training_Data_Target_01	46.919500	46.905612	-96.770016	-96.794248	-96.782279, 46.912921
Training_Data_Target_02	46.863251	46.851421	-96.799174	-96.813933	-96.80588, 46.857319
Training_Data_Target_03	46.841892	46.835658	-96.811610	-96.814912	-96.813458, 46.83868
Training_Data_Target_04	46.897152	46.893342	-96.782442	-96.787731	-96.785371, 46.895122

Feature:	Relative Risk Calculation:
Roads A1	

Disease Status

		Cases	Controls	Totals	Relative Risk	Lower 95% CI	Upper 95% CI
Exposure Status	< 1 km	135	1349	1484	2.11	1.75	2.55
	1 - 2 km	64	399	463	3.01	2.36	3.84
	2 - 5 km	116	1006	1122	1.92	1.58	2.34
	5 - 10 km	78	1325	1403	0.776	0.614	0.981
	10 - 20 km	36	2237	2273	0.128	0.091	0.179
	> 20 km	80	3351	3431	0.023	0.018	0.029
	Totals	509	9667	10176			

Feature:	Relative Risk Calculation:
Roads A2	(see table below)

		Disease Status					
		Cases	Controls	Totals	Relative Risk	Lower 95% CI	Upper 95% CI
Exposure Status	< 1 km	1	55	56	0.356	0.051	2.49
	1 - 2 km	5	88	93	1.08	0.457	2.53
	2 - 5 km	36	315	351	2.10	1.52	2.90
	5 - 10 km	67	835	902	1.48	1.16	1.90
	10 - 20 km	65	2170	2235	0.435	0.337	0.563
	> 20 km	335	6204	6539	0.051	0.043	0.061
	Totals	509	9667	10176			

Feature:	Relative Risk Calculation:
Roads A3	

		Disease Status				
		Cases	Controls	Totals	Lower 95% CI	Upper 95% CI
Exposure Status	< 1 km	352	5706	6058	1.27	1.83
	1 - 2 km	91	2126	2217	0.626	0.976
	2 - 5 km	55	1735	1790	0.028	0.049
	5 - 10 km	11	100	111	0.056	0.175
	10 - 20 km	0	0	0		
	> 20 km	0	0	0		
	Totals	509	9667	10176		

Feature:	Relative Risk Calculation:
Roads A5	

		Disease Status					
		Cases	Controls	Totals	Relative Risk	Lower 95% CI	Upper 95% CI
Exposure Status	< 1 km	19	225	244	1.578	1.02	2.45
	1 - 2 km	15	318	333	0.898	0.543	1.48
	2 - 5 km	52	1212	1264	0.753	0.569	0.998
	5 - 10 km	66	1873	1939	0.498	0.386	0.642
	10 - 20 km	135	3151	3286	0.358	0.296	0.434
	> 20 km	222	2888	3110	0.071	0.060	0.085
	Totals	509	9667	10176			

Feature:	Relative Risk Calculation:
Roads A71	see table below

		Disease Status					
		Cases	Controls	Totals	Relative Risk	Lower 95% CI	Upper 95% CI
Exposure Status	< 1 km	36	74	110	6.96	5.25	9.23
	1 - 2 km	39	100	139	5.99	4.53	7.93
	2 - 5 km	98	517	615	3.64	2.97	4.47
	5 - 10 km	91	923	1014	1.81	1.46	2.26
	10 - 20 km	70	2174	2244	0.449	0.350	0.575
	> 20 km	175	5879	6054	0.029	0.024	0.035
	Totals	509	9667	10176			

Feature:	Relative Risk Calculation:
Rails B1	

		Disease Status					
		Cases	Controls	Totals	Relative Risk	Lower 95% CI	Upper 95% CI
Exposure Status	< 1 km	170	1976	2146	1.88	1.57	2.24
	1 - 2 km	139	1481	1620	1.98	1.64	2.39
	2 - 5 km	164	3119	3283	0.498	0.415	0.596
	5 - 10 km	32	2238	2270	0.039	0.028	0.056
	10 - 20 km	4	684	688	0.008	0.003	0.021
	> 20 km	0	169	169			
	Totals	509	9667	10176			

Feature:	Relative Risk Calculation:
Rails B2	

		Disease Status					
		Cases	Controls	Totals	Relative Risk	Lower 95% CI	Upper 95% CI
Exposure Status	< 1 km	34	320	354	1.99	1.43	2.77
	1 - 2 km	66	498	564	2.54	1.99	3.24
	2 - 5 km	178	1970	2148	1.81	1.51	2.15
	5 - 10 km	138	3236	3374	0.443	0.366	0.536
	10 - 20 km	93	2916	3009	0.085	0.068	0.106
	> 20 km	0	727	727			
	Totals	509	9667	10176			

Feature:	Relative Risk Calculation:

Ash Basal Area

0 – 0.63

(m^2/ha)

Disease Status

Exposure Status		Cases	Controls	Totals	Relative Risk	Lower 95% CI	Upper 95% CI
	< 1 km	507	9657	10164	0.299	0.084	1.06
	1 - 2 km	0	0	0			
	2 - 5 km	0	1	1			
	5 - 10 km	0	0	0			
	10 - 20 km	2	9	11	0.182	0.052	0.639
	> 20 km	0	0	0			
	Totals	509	9667	10176			

Feature:	Relative Risk Calculation:
Ash Basal Area 0.63 – 2.53 (m^2/ha)	See table below

Disease Status

Exposure Status		Cases	Controls	Totals	Relative Risk	Lower 95% CI	Upper 95% CI
	< 1 km	499	9529	10028	0.736	0.402	1.35
	1 - 2 km	8	114	122	1.32	0.670	2.59
	2 - 5 km	0	15	15			
	5 - 10 km	0	0	0			
	10 - 20 km	2	9	11	0.182	0.052	0.639
	> 20 km	0	0	0			
	Totals	509	9667	10176			

Feature:	Relative Risk Calculation:
Ash Basal Area 2.53 – 5.90 (m^2/ha)	see table below

		Disease Status					
		Cases	Controls	Totals	Relative Risk	Lower 95% CI	Upper 95% CI
Exposure Status	< 1 km	422	7864	8286	1.11	0.883	1.39
	1 - 2 km	77	1247	1324	1.19	0.943	1.51
	2 - 5 km	8	500	508	0.018	0.009	0.035
	5 - 10 km	0	47	47			
	10 - 20 km	2	9	11	0.182	0.052	0.639
	> 20 km	0	0	0			
	Totals	509	9667	10176			

Feature:	Relative Risk Calculation:
Ash Basal Area 5.90 – 11.6 (m^2/ha)	

Disease Status

Exposure Status		Cases	Controls	Totals	Relative Risk	Lower 95% CI	Upper 95% CI
	< 1 km	255	3867	4122	1.47	1.245	1.75
	1 - 2 km	142	2729	2871	0.984	0.815	1.19
	2 - 5 km	108	2178	2286	0.152	0.124	0.188
	5 - 10 km	2	577	579	0.006	0.001	0.022
	10 - 20 km	2	314	316	0.006	0.002	0.025
	> 20 km	0	2	2			
	Totals	509	9667	10176			

Feature:	Relative Risk Calculation:
Ash Basal Area 11.6 – 54.0 (m^2/ha)	See table below

		Disease Status					
		Cases	Controls	Totals	Relative Risk	Lower 95% CI	Upper 95% CI
Exposure Status	< 1	110	1319	1429	1.69	1.38	2.07
	1 - 2 km	134	1474	1608	1.90	1.57	2.30
	2 - 5 km	187	3391	3578	0.618	0.518	0.736
	5 - 10 km	69	1986	2055	0.148	0.115	0.190
	10 - 20 km	7	1013	1020	0.013	0.006	0.028
	> 20 km	2	484	486	0.004	0.001	0.016
	Totals	509	9667	10176			

Feature:	Relative Risk Calculation:
Campgrounds < 65 RV Sites	

Disease Status

Exposure Status	Cases	Controls	Totals	Relative Risk	Lower 95% CI	Upper 95% CI
< 1 km	0	25	25			
1 - 2 km	1	62	63	0.316	0.045	2.213
2 - 5 km	16	333	349	0.906	0.557	1.47
5 - 10 km	38	890	928	0.767	0.555	1.06
10 - 20 km	138	2592	2730	0.836	0.691	1.01
> 20 km	316	5765	6081	0.052	0.044	0.062
Totals	509	9667	10176			

Feature:	Relative Risk Calculation:
Campgrounds < 65 RV Sites	

		Disease Status					
		Cases	Controls	Totals	Relative Risk	Lower 95% CI	Upper 95% CI
Exposure Status	< 1 km	0	25	25			
	1 - 2 km	1	62	63	0.316	0.045	2.213
	2 - 5 km	16	333	349	0.906	0.557	1.47
	5 - 10 km	38	890	928	0.767	0.555	1.06
	10 - 20 km	138	2592	2730	0.836	0.691	1.01
	> 20 km	316	5765	6081	0.052	0.044	0.062
	Totals	509	9667	10176			

Feature:	Relative Risk Calculation:
Campgrounds 65 - 120 RV Sites	

		Disease Status					
		Cases	Controls	Totals	Relative Risk	Lower 95% CI	Upper 95% CI
Exposure Status	< 1 km	4	45	49	1.64	0.638	4.20
	1 - 2 km	19	74	93	4.20	2.79	6.34
	2 - 5 km	57	307	364	3.36	2.60	4.33
	5 - 10 km	44	780	824	1.03	0.759	1.38
	10 - 20 km	130	2524	2654	0.816	0.672	0.991
	> 20 km	255	5937	6192	0.041	0.035	0.049
	Totals	509	9667	10176			

Feature:	Relative Risk Calculation:
Campgrounds 121 - 175 RV Sites	(see table below)

		Disease Status					
		Cases	Controls	Totals	Relative Risk	Lower 95% CI	Upper 95% CI
Exposure Status	< 1 km	3	31	34	1.77	0.598	5.23
	1 - 2 km	6	54	60	2.01	0.937	4.32
	2 - 5 km	10	252	262	0.762	0.412	1.41
	5 - 10 km	15	669	684	0.406	0.245	0.675
	10 - 20 km	85	2184	2269	0.610	0.485	0.766
	> 20 km	390	6477	6867	0.057	0.046	0.069
	Totals	509	9667	10176			

Feature:	Relative Risk Calculation:
Campgrounds 176 - 240 RV Sites	see table below

		Disease Status					
		Cases	Controls	Totals	Relative Risk	Lower 95% CI	Upper 95% CI
Exposure Status	< 1 km	0	39	39			
	1 - 2 km	0	89	89			
	2 - 5 km	0	299	299			
	5 - 10 km	27	818	845	0.590	0.038	0.403
	10 - 20 km	56	2151	2207	0.377	0.019	0.286
	> 20 km	426	6271	6697	0.064	0.014	0.050
	Totals	509	9667	10176			

Feature:	Relative Risk Calculation:
Campgrounds > 240 RV Sites	See table below

Disease Status

Exposure Status		Cases	Controls	Totals	Relative Risk	Lower 95% CI	Upper 95% CI
	< 1 km	1	55	56	0.356	0.051	2.49
	1 - 2 km	5	88	93	1.08	0.457	2.53
	2 - 5 km	36	315	351	2.10	1.52	2.90
	5 - 10 km	67	835	902	1.48	1.16	1.90
	10 - 20 km	65	2170	2235	0.435	0.337	0.563
	> 20 km	335	6204	6539	0.051	0.043	0.061
	Totals	509	9667	10176			